UNIVERSITÀ DEGLI STUDI DEL PIEMONTE ORIENTALE

"AMEDEO AVOGADRO"

Tesi di Dottorato di Ricerca in MEDICINA MOLECOLARE

XXVI CICLO

CHARACTERIZATION OF MOLECULAR MECHANISMS INVOLEVED IN MESOHELIOMA CARCINOGENESIS AND IDENTIFICATION OF NEW BIOMARKERS FOR TREATMENT SELECTION.

Coordinatore:

Prof. Emanuele Albano

Supervisore:

Prof. Renzo Boldorini

Dottorando:

Rosanna Mezzapelle

Table of Contents

1 INTRODUCTION

1.1 Malignant Mesothelioma

Mesothelial cells form the serosal lining of the pleural, pericardial and peritoneal cavities. Among the most undifferentiated cells of our body mesothelial cells are able to differentiate morphologically into epithelial-like cells or fibroblast-like cells. (Carbone *et al*, 2002) Malignant mesothelioma is a rare but very aggressive tumour which arises from the mesothelial cells; the pleural subtype is the most frequent (80%) (Boutin *et al*.,1998). Malignant pleural mesothelioma (MPM) is strongly related to asbestos and/or asbestos-like fibers exposure, moreover MPM etiology is linked to Simian virus 40 infection, radiation and genetic susceptibility. MPM is characterized by a long latency (interval between first exposure to risk factors and the development of the pathology) that ranges from 10 to 45 years. The incidence of MPM in Italy is 2,94/100.000 for men and 1,06/100.000 for women. In those areas in which there were asbestos production factories, like for example Casale Monferrato in Piedmont region, the incidence rises to 43.7/100.000 for men and 27/100.000 for woman (Centro di Riferimento per l'Epidemiologia e la Prevenzione Oncologica in Piemonte). According to epidemiologic studies, it is estimated that MPM mortality rates will continue to increase by 5-10% per year in most industrialized countries for the next 2-3 decades, despite asbestos abatement efforts. In Italy the peak will be reach in 2015 (Peto J. *et al,* 1999) (Figure 1).

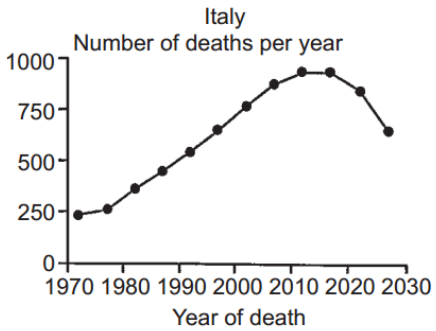

Figure 1. Observed (to 1989) and predicted (1990–2029) annual numbers of pleural cancer deaths in men in Italy.

Prognosis of MPM is poor, the overall survival in no treated patients ranges from 4 to 12 months. (Pass et al.,2001). According to the amount of epithelial and spindle cells we can distinguish three histologic subtypes: epithelioid, sarcomatoid and biphasic (Figure 2); they are associated with a

different prognosis. The epithelioid subtype is considered the least aggressive and most responsive to treatments, with the best prognosis (Boutin *et al*, 1998; Robinson *et al.*,2005).

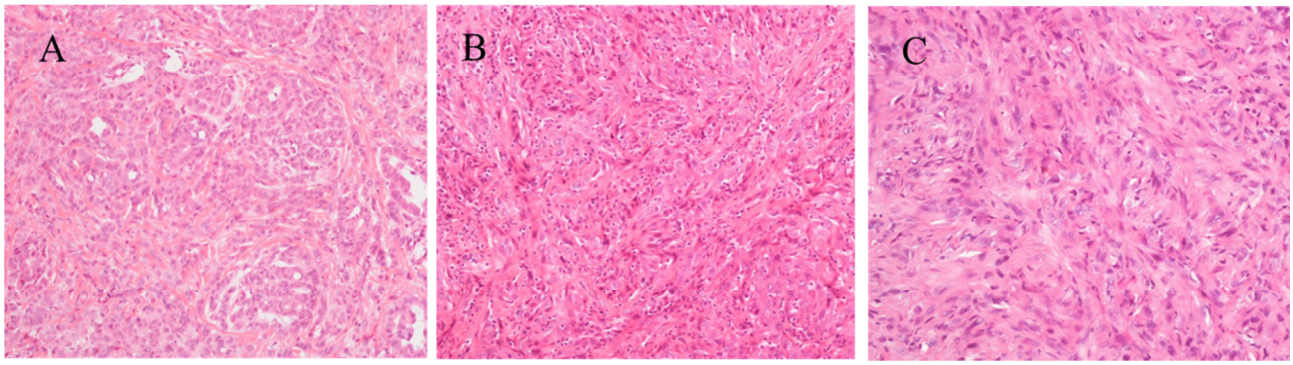

Figure 2 Example of histologic subtypes of MPM: A) Epithelioid B) Biphasic C) Sarcomatoid. *Magnification 200X*

1.2 Etiology and Pathogenesis

1.2.1 Asbestos and Mesothelioma

Prior to the 1950s, malignant mesotheliomas were extremely rare. The first documented case of mesothelioma, according to current diagnostic criteria, was published in 1947. Asbestos is a generic name for a family of naturally silicate minerals with different carcinogenicities (Mossman *et al*, 1990). The various types of asbestos are divided into two major groups: serpentine represented by crysotile, the most common and economically important form of asbestos in the Western World; and the amphiboles, which include crocidolite, the most oncogenic type of asbestos, amosite, anthophyllite, and tremolite. The link between asbesotos fibers and MPM development is well established (Boutin *et al*, 1996; Boffetta *et al*, 2007), moreover Fang *et al*. recently showed how chrysotile can cause transformation in human mesothelial cells via HMGB1 and TNF-α signaling (Qi *et al*, 2013). Amphibole are very thin fibers (diameter 3μm) which have the capacity to reach the pleura either through the lymphatic, or by direct penetration and to cause fibrosis, pleural plaques, and eventually mesothelioma. Moreover they can damage the mitotic spindle of the cell leading to aneuploid and DNA damage. (Ault *et al*, 1995; Kamp *et al*, 1995). A key mechanism by which asbestos causes the transformation of mesothelial cells has recently been elucidated: working with primary human mesothelial (HM) cells, Yang et al discovered that asbestos induces necrotic cell death with resultant release of HMGB-1 in the extra cellular space. HMGB-1 release causes a chronic inflammatory response, macrophage accumulation and the secretion of TNF-α, which in turn activates NF-kB, leading to the survival of HM cells that have accumulated genetic damage because of asbestos exposure (Figure 32) (Yang *et al*, 2010).

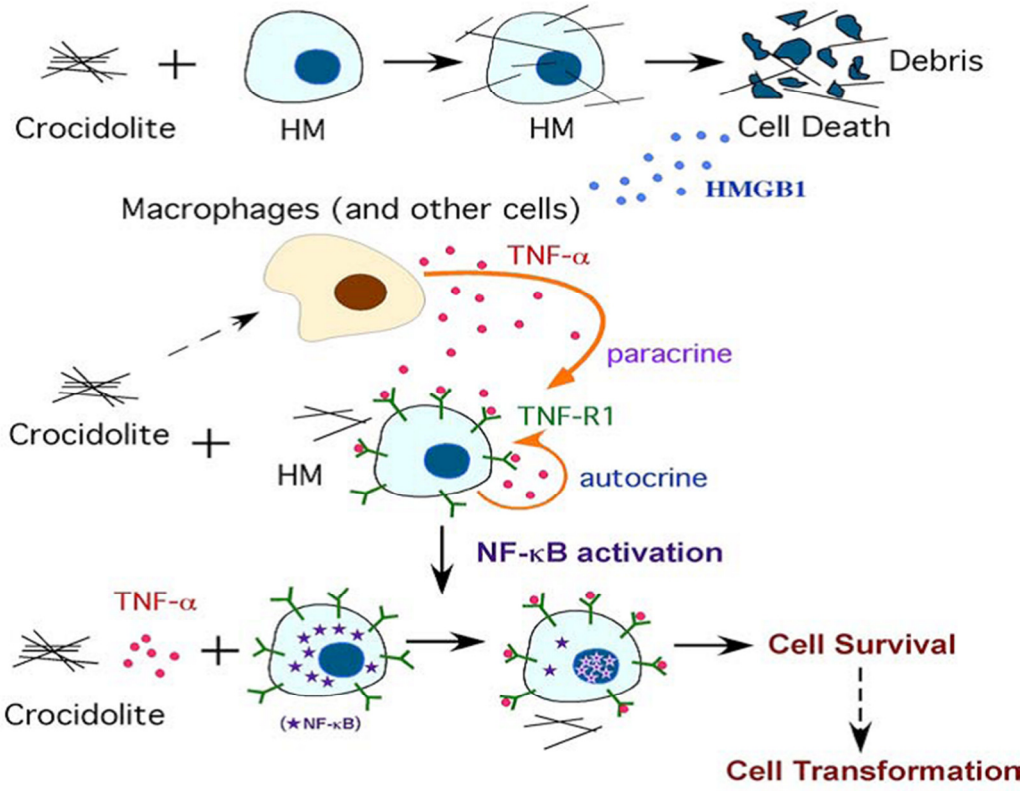

***Figure 3** Mechanism of asbestos-induced pathogenesis.*

Erionite is an asbestos-like mineral more carcinogenic than asbestos to induce mesothelioma (Hill *et al*, 1990); Wagner and colleagues showed that mice injected with erionite develop MM in almost all cases, instead mice injected with asbestos fibers has MM in a lower percentage of cases (48%) (Wagner *et al*, 1985). In a recent work Carbone linked erionite with endemic cases of mesothelioma in some Turkish villages of Cappadocia (erionite is natural component of the stones of this region) and in North and South Dakota, showing that it is a serious cause of environmental pollution (Carbone *et al*, .2011). Some studies have shown that asbestos exposure causes activation of MAPK, phosphatidylinositol-3-kinase (PI3K)-AKT and the downstream mTOR (the target for rapamacyin) in MM (Altomare DA et al., 2005; Wilson SM et al., 2008).

1.2.2 SV40 and mesothelioma

Simian Virus 40 is a normal guest of macaque species of monkeys, it is a double circle DNA virus with two coding regions: early and late according to which is first coded. Early region codes T antigen (large T antigen) and t antigen (small t antigen). The ability to induce tumor transformation in the host cells is linked to the large T antigen, indeed it binds and inactivates essential tumor suppressor genes, like p53 and pRb, stimulates Met, Notch-1 and telomerase activity. (Carbone *et*

al, 1997; De Luca *et al,* 1997; Caciotti *et al,* 2001; Bocchetta *et al.,* 2003; Foddis *et al*, 2002). Hamsters intracardially injected with SV40 develop MM in the 60% of cases (6-9 months), as well as intrapleurally injected mice show MM in the 100% of cases (4-6months) (Cicala *et al,* 1993). In the 60'-70', millions of people worldwide were injected with the inactivated (Salk) and early live attenuated (Sabin) forms of polio vaccines that were contaminated with SV40, however its ability to cause tumour in human is not very clear since several conflicting data have been reported.

1.2.3 Genetic predisposition

Some individuals develop mesothelioma following exposure to small amounts of asbestos, whereas others exposed to heavy amounts do not. Carbone et al. have reported mesothelioma clustering in some US and Turkish families in which up to 50% of members developed mesothelioma (Carbone *et al*, 2007). This incidence far exceeds that observed in cohorts exposed to high levels of asbestos (4.6%), suggesting a genetic predisposition. Carbone et al. focused on two American families with high incidence of mesothelioma to identify putative mesothelioma susceptibility genes. The members of these families were neither exposed to erionite nor had occupational exposure to asbestos, thus removing the confounding factor of heavy exposure to carcinogens known to cause a high incidence of mesothelioma. Family members developed various malignancies, although mesothelioma predominated (Testa *et al*, 2001). Array-comparative genomic hybridization (CGH) analysis of two tumors (one per family) uncovered alterations encompassing or adjacent to the BAP1 (BRCA-1 associated protein 1) locus at 3p21.1. Beside mesothelioma development BAP1 germline mutations have been also liked to uveal melanoma and to a type of benign melanocytic tumors that called mBAITS5 (melanocytic BAP1-mutated atypical intradermal tumours (Carbone *et al*, 2013).

1.2.4 Radiation

Radiation exposure has also been linked to MM, even though these cases are rarely observed (Goodman *et al*, 2009). Patients who received radiation treatments, specifically in the thoracic or abdominal regions, or who received Thorotrast intravascularly have shown increased risks in developing MM (Amin *et al*, 2001). Moreover, studies in rats demonstrate that radiation is a causative co-factor of MM in combination with asbestos exposure (Lafuma *et al*, 1980).

In summary, the association between asbestos, erionite, SV40 infection, genetic predisposition and radiation exposure suggests a multifactorial origin for malignant mesothelioma and each factor plays a crucial role in necrosis, inflammation and genetic damage.

1.3 Clinical features

The mean age at presentation is 60 years because of the long latency from the time of first exposure to asbestos to the development of clinically evident disease (Britton M., 2002). The incidence is higher in men, presumably because more men have worked in asbestos-related trades. Symptoms and physical findings are generally not specific for the disease. Most patients present with non-pleuritic chest pain or dyspnea. Compared to that of metastatic pleural diseases, the pain from mesothelioma can be severe, aching, and often very difficult to control. Less common complaints are cough, fevers, chills, sweats, and fatigue. Fatigue, cachexia and pain are common in advanced disease. Physical examination is usually only remarkable for signs related to the presence of a pleural effusion or mass. Later in the course of disease one can often appreciate volume loss and decreased mobility of the chest wall on the side of the primary tumor. Occasionally, the tumor may extend directly into the chest wall, and be detected as a tender or non-tender chest wall mass.

1.4 Diagnosis

Diagnosis of malignant mesothelioma requires a careful evaluation of the clinical and radiological features, and it must be confirmed by a pleural biopsy.
The main radiologic technics used to diagnose mesothelioma are:

- **Computer Tomography (TAC)** TAC is able to detect pleural effusion, pleural thickening, calcification, intralobular thickening and the potential thoracic invasion. However TAC cannot distinguish between benign tumour, adenocarcinoma and mesothelioma. TAC scanning may help fine needle aspiration/biopsy of pleural mass.
- **Magnetic resonance Imaging (MRI)** MRI scanning allows to determine tumour size and to better detect the tumor area and distinguish the normal part. MRI is more accurate than TAC to evaluate the mediastinic lymphonodal enlargement.

- **Positron emission tomography (PET)** PET imaging is a nuclear technique that produces three-dimensional image, it is currently the better way to locate the onset tumor sites. Fluorodeoxyglucose positron emission tomography (PET) and particularly PET/CT shows promise as a tool to differentiate benign from malignant disease and as an adjunctive tool for staging. A combination of the imaging techniques may be necessary for determining the best approach to the patient (Wang *et al*, 2004).

Histology

In order to obtain a definitive diagnosis of MPM the tissue biopsy and/or pleural effusion exams are essential. The pleural effusion often shows high level of bloody cells, high protein concentration, low level of white cells and low PH. The high content of hyaluronic acid is suggestive of mesothelioma, but it is poorly specific, so the cytologic analysis, as well as the trans-needle aspiration rarely lead to a definite diagnosis. The histologic evaluation of pleural biopsy is therefore of crucial support to the diagnosis. However, in many cases, to confirm the MPM diagnosis it's necessary to investigate a panel of tumoral markers by the mean of immunohistochemistry. According to the embryologic histogenesis of mesothelial tissue, MPM shows epithelial and mesothelial markers such as cytocheratin 5/6, carletinin, thrombomodulin, mesothelin and the Wilms Tumor 1 (WT-1). The presence of at least two of positive markers in the context of a clinical and histological suspicion, is sufficient to confirm the diagnosis of MPM (Chierieac *et al,* 2009). Very often the diagnosis of MPM occurs in its late stage. TNM-based staging system by the International Mesothelioma Interest is the most widely used staging system for MPM (Rusch, 1995), it can be summarized as in Figure 4.

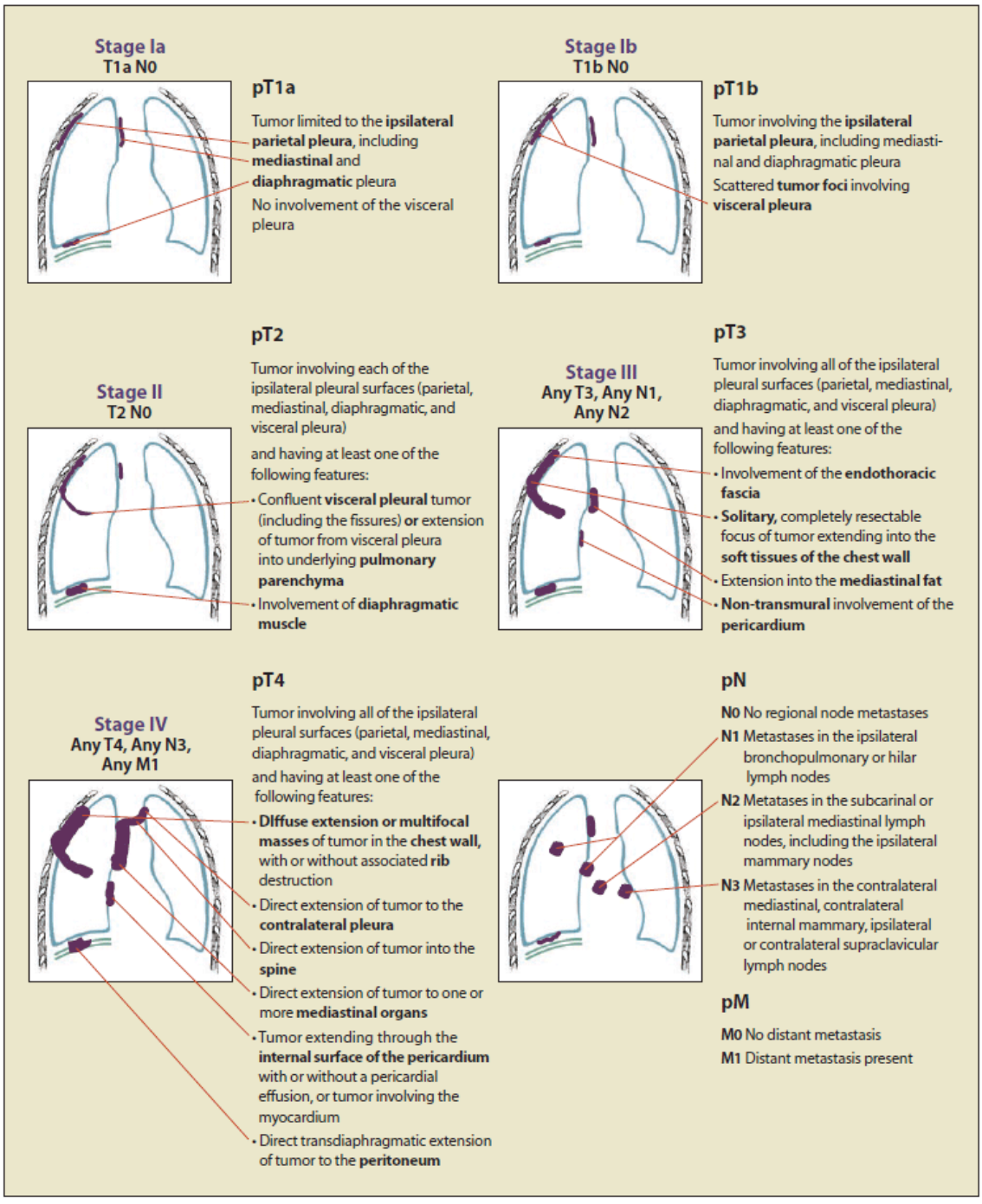

Figure 4 *IMIG Staging System for Malignant Pleural Mesothelioma.*

1.5 Therapy

There are no therapeutic standards for malignant mesothelioma and the treatment options depend on performance status, pulmonary function, stage, and age of the patient.

1.5.1 Surgery

The two potential goals of surgical therapy for pleural mesothelioma are palliation of symptoms and debulking of tumor with therapeutic intent. For surgical debulking of mesotheliomas, two surgical approaches are commonly employed, pleurectomy with decortication (P/D) or extrapleural pneumonectomy (EPP). Pleurectomy with decortication (P/D) removes all gross disease from all pleural surfaces and preserves the underlying lung. Extrapleural pneumonectomy (EPP) entails en bloc removal of the lung along with surrounding parietal pleura, pericardium, and diaphragm, with the pericardium and diaphragm then replaced by synthetic grafts. These are both technically challenging procedures and should be performed only by surgeons with extensive experience. EPP is especially difficult, and was originally associated with an unacceptably high morbidity of 30%. However, with advances in surgical, anesthetic, and critical care techniques, and more exacting patient selection, experienced centers now report mortality rates of < 4%, a rate comparable to standard pneumonectomy (Sugarbaker *et al*, 1999).

1.5.2 Radiation therapy

Although in vitro studies suggest that mesothelioma is more sensitive to radiation than non-small cell lung cancer (Charmichael *et al*, 1989), the clinical experience reported by radiation oncologists suggests that it is an especially radio-resistant tumor. In addition, radiation of the involved chest is limited by the presence of radiosensitive organs and the extensive nature of the tumor. As a consequence, its use appears limited to adjunctive therapy for patients who have undergone EPP, and to palliative treatment of painful chest wall lesions. Prophylactic chest wall irradiation may reduce the incidence of chest wall recurrences at incision sites but there is no consensus on its use and randomized controlled trials are needed (Lee *et al*, 2009). An area of active ongoing research is the role of high-dose hemithorax irradiation after extrapleural pneumonectomy for early stage disease. In carefully staged patients, this approach has resulted in a marked reduction in local tumor recurrences, although nearly one half of patients subsequently developed isolated distant metastases (Senan *et al*, 2003).

1.5.3 Chemotherapy

Most patients with mesothelioma are not candidates for surgical or radiotherapy treatment and chemotherapy is their main option. The most commonly regimen used now includes the multitargeted antifolate drug pemetrexed with a platinum drug such as cisplatinum. The use of this combination has been compared to cisplatin alone in a large Phase III study of 456 patients (Vogelzang *et al*, 2003). Response rates were significantly better in the pemetrexed/cisplatin arm

than in the cisplatin alone arm (41.3% vs. 16.7%), and survival was significantly better as well (median survival 12.1 months versus 9.3 months). Addition of folic acid and vitamin B12 significantly reduced toxicity without altering survival benefit. The other regimen used commonly is the false nucleotide gemcitabine with a platinum agent. Nearly half of the patients on this doublet regimen noted symptom improvement, 33% had a partial response, and 60% had stable disease; no survival benefit was demonstrated compared to historical controls (Novak *et al*, 2002). Similarly, treatment with the combination of gemcitabine and oxaliplatin has been reported to improve symptoms, but not significantly improve survival (median survival of 13 months) (Schutte *et al*, 2003). Platinum compounds act through the formation of platinum-DNA adducts. Removal of these adducts, which leads to chemoresistance, is mainly carried out by the nucleotide excision repair (NER) system that consists of at least 30 identified polypeptides, including the pivotal protein excision repair cross-complementing group-1 (ERCC1) (Sancar A., 1995). It is hypothesized that low expression of ERCC1 might predict increased sensitivity to platinum-based chemotherapy, possibly due to the saturation of the enzyme complex; conversely, high levels of ERCC1 may predict a resistance to platinum-based chemotherapy. Pemetrexed (commercial name *Alimta®*), is a multitargeted antifolate agent that inhibits dihydrofolate reductase (DHFR), thymidylate synthase (TS), and glycinamide ribonucleotide formyltransferase (GARFT), enzymes involved in purine and pyrimidine synthesis. However, pemetrexed is a weak inhibitor of GARFT, and when TS is inhibited, tetrahydrofolate oxidation stops and there is no longer a need for DHFR activity (Chattopadhyay *et al*, 2007). Therefore, most studies have focused on pemetrexed effects on TS. TS mRNA levels were inversely correlated with pemetrexed activity in different tumor cells (Hanauske *et al*, 2007; Giovannetti *et al*,2008), whereas other studies suggested a correlation between high levels of TS protein expression and reduced sensitivity to pemetrexed in colon and lung cancer cells (Sigmond *et al*, 2003).

1.5.4 Immunotherapy

It is known that an immune response is induced by mesothelioma, but it is weak (Robinson *et al,* 2000). This knowledge has prompted a number of investigators to study different ways to consolidate that response. The intrapleural instillation of cytokines is limited by the short half-life of most cytokines, necessitating repeated injections or continuous infusion via a pleural catheter. Intrapleural interferon-gamma twice weekly for 2 months was reported to induce response rate of 56% in early stage disease (Boutin *et al*, 1991). A continuous intrapleural infusion of interleukin-2 induced a partial response in four of 21 patients and an overall survival of 16 months (Goey *et al*, 1995). In both cases, side effects were minimal and consisted primarily of fever and constitutional

symptoms. Studies in animals suggest that interferons have an antiproliferative effect on mesothelioma cells and enhance the cytotoxic effect of cisplatin. The results from these studies led to the development of a Phase II trial of cisplatin-doxorubicin and interferon alpha-2 in advanced maligant mesothelioma. The overall response rate was 29% and the median survival was 9.3 months with a one year survival of 45% and two year of 34% (Parra *et al*, 2001). However, severe myelosuppression was seen in 60% of patients limiting the application of this treatment.

1.5.5 New agent under study

Studies of the molecular biology of mesothelioma and the cellular mechanisms leading to a malignant phenotype have led to the identification of several possible therapeutic targets for treatment of this disease. Some of these are already under investigation in clinical trials, for example, several receptor tyrosine kinases are aberrantly expressed in these tumors, including the epidermal growth factor receptor (EGFR) (Janne *et al*, 2002). Inhibitors of these proteins are now available in oral form and are being evaluated in patients with mesothelioma. Other novel agents targeting growth factors found to be overexpressed in mesothelioma, e.g. vascular endothelial growth factor and its receptor, are under investigation. Other agents under study include anti-angiogenic agents, e.g. AZD2171, thalidomide and PTK/ZK787, inhibitors of histone deacetylase superoylanilide and hydroxamic acid (SAHA), proteasome inhibitors, and histone deacetylase inhibitors (PXD101). Furthermore, two classes of EGFR antagonists, small molecule tyrosine kinase inhibitors (TKIs) and monoclonal antibodies (mAbs), have been approved by the Food and Drug administration (FDA) and the European Medicines Evaluation Agency (EMEA) for the treatment of metastatic NSCLC, colorectal cancer (mCRC), squamous-cell carcinoma of the head and neck and pancreatic cancer (Gridelli *et al*, 2007; Sridhar *et al,* 2003). Gefitinib and erlotinib, two reversible TKIs, inhibit the EGFR phosphorylation and its downstream cascade by blocking the ATP pocket located in the intracellular catalytic domain of the receptor. Cetuximab and panitumumab, two anti-EGFR mAbs, target the extracellular domain of the receptor and upon the receptor binding they inhibit its dimerization and subsequent phosphorylation and signal transduction (*Figure 5*). The introduction of cetuximab and panitumumab in clinical practice, either in combination with chemotherapy or as single agent, has shown to improve the outcome of metastatic CRC and NSCLC patients (Saltz *et al*, 2004). Preclinical studies have shown that EGFR TKIs are highly efficacious in mesothelioma cell cultures (Barbieri *et al*, 2011), but two phase II studies of gefitinib and erlotinib used alone to treat malignant pleural and peritoneal mesotheliomas failed to demonstrate their clinical efficacy. However it needs to be pointed out that the patients in both trials were not selected on the basis of any molecular criteria (Govindan *et al*, 2005; Garland *et*

al, 2007). One recent study has shown that cetuximab effectively blocks the growth of MPM cells in cell cultures and mouse models (Kurai *et al*, 2012) and, as in the case of colorectal cancer and lung adenocarcinomas, the potential efficacy of these TKIs in MPM may depend on the mutation status of EGFR gene and its downstream effectors (Lie`vre *et al,* 2006). To the best of our knowledge, only a few low-powered studies have investigated the presence and frequency of EGFR gene mutations in MPM (Cortese *et al*, 2006; Enomoto *et al,* 2012), and none has searched for mutations in the KRAS, BRAF, and PI3KCA downstream effectors.

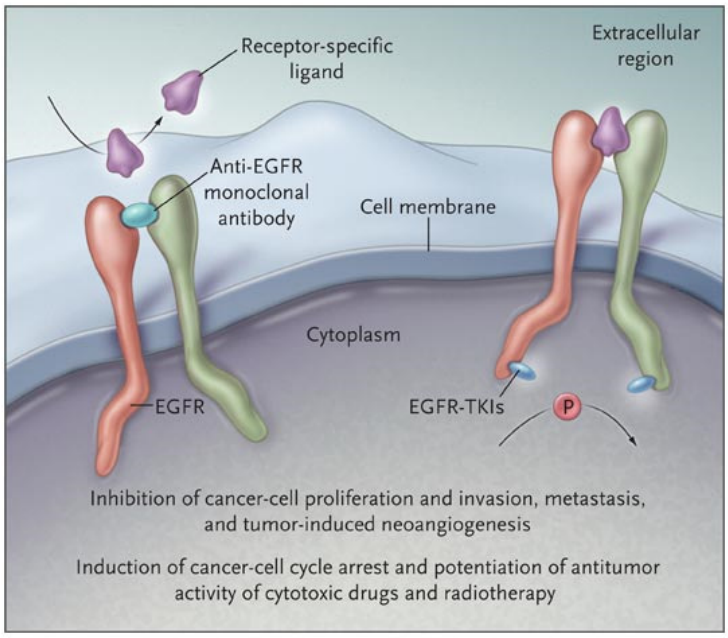

Figure 5 EGFR inhibitors, mAbs and TKIs

1.6 Epidermal growth factor receptor (EGFR).

Epidermal growth factor (EGF) was first discovered by Stanley Cohen in 1960 during his study of nerve growth factor in mouse sub-maxillary glands and subsequently, in 1975, he confirmed the presence of plasma membrane receptors in human fibroblasts (Cohen *et al*, 1960, Carpenter *et al*, 1975). EGFR was isolated in 1982 as a 170 kDa transmembrane glycoprotein with an EGF binding site on the extracellular surface (Cohen *et al,* 1982). The structure of EGFR was found to be the human equivalent of the mammalian v-erb-B oncogene protein from the avian erythroblastosis virus. Unlike the human EGFR, the v-erb-B oncogene protein did not have the extracellular EGF binding domain thereby demonstrating that the intracellular domain may play an important role in tumourigenesis. EGFR belongs to the human epidermal growth factor receptor (HER) family, which

has four structurally related receptor tyrosine kinases. The EGFR gene localized on chromosome 7 p11-13, the protein consists of 1186 amino acids. The receptor structure consists of extracellular, transmembrane and intracellular domains. The extracellular domain consists of cysteine-rich clusters, which form the ligand-binding domain. Upon binding with ligands such as EGF or transforming growth factor alpha (TGF-α), the EGFR monomers form homodimers with another EGFR or heterodimers with another receptor of the HER family. The intracellular domain has tyrosine kinase activity. Dimerisation of the EGFR results in structural rearrangement of the intracellular tyrosine kinase domain, adenosine triphosphate (ATP) is then recruited into the catalytic domain, resulting in its auto-phosphorylation. This leads to the activation of a cascade of intracellular signal transduction pathways resulting in cell proliferation, anti-apoptosis, invasion and metastasis (Citri *et al*, 2006; Hynes *et al*, 2005; Bogdan *et al,* 2011). Among a host of various intracellular signalling pathways stimulated by EGFR, the major pathways activated are the RAS/RAF/MAPK pathway resulting in cell proliferation, metastasis and invasion, and the PI3K/AKT/mTOR pathway resulting in inhibition of apoptosis (Ciardello *et al*, 2008) (Figure 6).

The first signaling cascade shown to be downstream of the EGFR was the Ras–mitogen-activated protein kinase or MAP kinase pathway. When the pathway is activated, the SOS guanine nucleotide exchange factor is recruited to the plasma membrane via the Grb2/Drk/Sem5 adapter protein. SOS stimulates the exchange of GTP for GDP on the small G-protein Ras. Subsequently activated Ras stimulates the MAP kinase pathway to promote cell proliferation. Phosphoinositide 3-kinase (PI3K) plays a crucial role in effecting alterations in a broad range of cellular functions in response to extracellular signals. A key downstream effector of PI3K is the serine-threonine kinase Akt which in response to PI3K activation, phosphorylates and regulates the activity of a number of targets including kinases, transcription factors and other regulatory molecules (Paez *et al*, 2000). The complexity of signaling is further increased by cross-talk between individual pathways. Since EGFR is associated with an oncogenic phenotype, its inhibition may result in an anti-neoplastic effect. As mentioned before, in the last decade several inhibitors of EGFR have been developed, including monoclonal antibodies (cetuximab) and small molecule inhibitors (gefitinib, erlotinib), which have been shown to be effective in animal models, in preclinical and clinical studies (Mendelsohn *et al*, 2003). A correlation between EGFR expression and response to therapy has been reported in some human cancers (breast, lung and prostate) (Santoro *et al*, 2004; Cappuzzo *et al*, 2003).

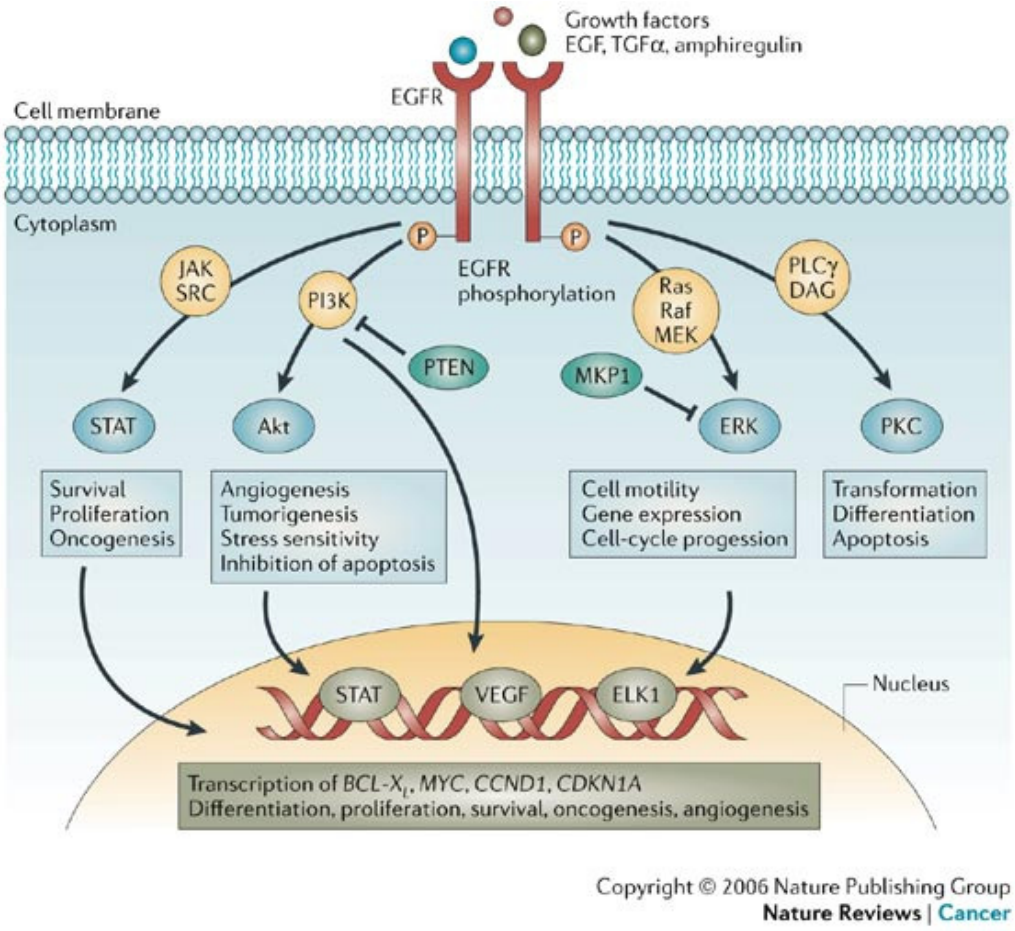

Figure 6 EGFR downstream signaling pathways

1.6.1 EGFR mutations and inhibitors

Activating EGFR mutations have been reported in cancers such as non-small-cell lung cancer (NSCLC) and head and neck cancers, and are predictive of the response to gefitinib or erlotinib therapy (Lynch *et al*, 2004; Paez *et al*, 2004; Lee *et al,* 2005). Approximately 90% of EGFR mutations affect small regions of the gene within exons (18 to 24) that code for the EGFR tyrosine kinase domain. The most common mutations are an in-frame deletion in exon 19 around codons 746 to 750 (accounting for 45 to 50% of EGFR mutations) and a missense mutation leading to a substitution of arginine for leucine at codon 858 (L858R) in exon 21 (35 to 45% of EGFR mutations) (Sharma *et al*, 2007). Somatic EGFR mutations are found in approximately 5 to 15% of unselected white patients and in 25 to 35% of unselected Asian patients with NSCLC. These mutations seem to be limited to NSCLC, since they have rarely been detected in other types of human cancer.

1.7 v-Ki-ras2 Kirsten rat sarcoma viral oncogene homolog (KRAS)

KRAS is a small GTPases that regulate cell growth, proliferation and differentiation, it is normally activated in response to the binding of extracellular signals, such as growth factors, RTKs (Receptor Tyrosine Kinases) and TCR (T-Cell Receptors). In the resting cell, KRAS is tightly bound to GDP (Guanosine Diphosphate); as a result of extracellular stimuli to cell membrane receptors the guanine nucleotide exchange factors (GEFs) release GDP and allow GTP (Guanosine Triphosphate) binding. In the GTP-bound form, KRAS interacts specifically with effector proteins, thereby initiating cascades of protein-protein interactions that may finally lead to cell proliferation. Active GTP-bound KRAS interacts with several effector proteins: among the best characterized are the Raf kinases and phosphatidylinositol 3-kinase (PI3K) (Hancock JF., 2003). KRAS gene is localized on chromosome 12. More than 95% of KRAS activating gene mutations occurs at codon 12 and 13 of exon 2. Less frequent mutations occurs at codon 61. KRAS activating mutations cause resistence to anti-EGFR mABs target therapies.

1.8 v-raf murine sarcoma viral oncogene homolog B1 (BRAF)

BRAF gene is localized on chromosome 7q34, it encodes the protein BRAF belonging to the raf/mil family of serine/threonine protein kinases. This protein plays a role in regulating the MAP kinase/ERKs signaling pathway, which affects cell division, differentiation, and secretion, in fact activated BRAF activates mitogen-activated protein kinase (MAPK) and extracellular-signal regulated kinase (ERK, MEK1 and MEK2) by serine phosphorylation. Mutations in *BRAF* gene are associated with cardiofaciocutaneous syndrome, a disease characterized by heart defects, mental retardation and a distinctive facial appearance. Mutations in this gene have also been associated with various cancers, including non-Hodgkin lymphoma, colorectal cancer, malignant melanoma, thyroid carcinoma, non-small cell lung carcinoma, and adenocarcinoma of lung. The highest frequency of BRAF mutations is in malignant melanoma. The most common mutation is a T to A nucleotide transversion leading to a V600E amino acid substitution within the activation segment of the Raf serine/threonine kinase gene product, increases the catalytic activity of B-Raf and leads to subsequent activation of MEK and ERK MAPKs (Davies *et al*, 2002: Pollock *et al*, 2003). Since constitutively active BRAF mutants commonly cause cancer by excessively signaling to cell growth, inhibitors of BRAF have been developed for both the inactive and active conformations of the kinase domain as cancer therapeutic candidates (Bollag *et al*, 2010; Wan *et al*, 2004). Sorafenib

and Vemurafenib are currently the two BRAF molecular inhibitors approved by the FDA for the treatment of primary liver and kidney cancer and for late stage melanoma.

1.9 Phosphoinositide 3- kinase (PI3K)

The class I PI3Ks catalyse the conversion of phosphatidylinositol-3,4-bisphosphate (PtdIns-4,5-P 2) to phosphatidylinositol-3,4,5- trisphosphate (PtdIns-3,4,5-P3). These specialized lipids serve to recruit pleckstrin homology (PH) domain-containing proteins such as the serine-threonine kinase Akt and PDK1 (phosphoinositide-dependent kinase 1) to the plasma membrane. After recruitment to the membrane, Akt is phophorylated and consequently activated, by PDK. In turn, Akt phosphorylates multiple proteins on serine and threonine residues. Through phosphorylation of these targets, Akt carries out its role as a key regulator of a variety of critical cell functions including glucose metabolism, cell proliferation and survival. The PI3K family comprises eight members divided into three classes according to their sequence homology and substrate preference. PI3K enzymatic structure shows a catalytic subunit (p110) associated with a regulatory one (p85). The catalytic subunit PI3KCA is encoded by a gene localized at chromosome 3p26.32. Mutations in the PIK3CA gene are not frequent in colon rectal cancer, occurring in about 15% of these tumours. PIK3CA mutations mainly occur in exons 9 and 20, with exon 9 showing the highest incidence (68.5% approximately). These mutations can be found in the same tumour together with KRAS and BRAF mutations, and this makes difficult to evaluate their own role in defining the sensitivity to anti-EGFR mAbs. (Benvenuti *et al*, 2008; Samuel et al, 2004; Di Nicolantonio et al., 2010).

1.10 Prognostic and predictive biomarkers.

In the majority of patients MPM is diagnosed in stage III/IV, and systemic therapy represents the only potential treatment option for most cases. The combination of platinum or cisplatin and pemetrexed represents the standard of care in the first-line treatment of MPM. Several studies carried out on NSCLC showed that protein and mRNA ERCC1 expression have a consistent prognostic and predictive value in patient treated with cipslatin (Olaussen *et al,* 2006; Zheng *et al,* 2007). Similarly, in NSCLC cell lines, high baseline *TS* gene expression levels confer resistance to pemetrexed and TS protein levels are correlated to pemetrexed efficacy in a variety of solid tumours (Gomez et al. 2006; Rose et al 2002; Zuceli et a, 2011; Righi et al, 2010). Due to the epithelioid phenotype of the most part of MPM it could be interesting to investigate the ERCC1 and TS

gene/protein expression in order to determine whether they can have a prognostic and/or predictive value in mesothelioma patients.

1.10.1 Excision repair cross-complementing group-1 (ERCC1)

Platinum compounds function by binding to DNA resulting in intrastrand or interstrand crosslinks, which disrupt the DNA structure. These lesions may interfere with base pairing and generally obstruct transcription and normal replication processes, ultimately leading to apoptosis. The nucleotide excision repair (NER) pathway is 1 of 5 recognized DNA repair pathways (mismatch repair, double-strand break repair, base excision repair and direct repair) that maintain DNA integrity and defend DNA against environmental damage. It is generally well accepted that each of the repair pathways identifies distinct lesion types (Hoeijmakers, 2001). NER has been identified to repair bulky, helix-distorting DNA lesions caused by UV light or chemicals, including platinum compounds. NER pathway acts through the recognition of DNA repair, followed by the formation of a complex to unwind the damage portion and excise it. Finally, the excised area is resynthesized and bound to the undamaged DNA, restoring the double helix. After the repair process is complete, the entire complex is disassembled. Excision repair cross-complementation group 1(ERCC1) protein functions within the repair complex as it heterodimers with the Xeroderma pigmentosum complementation group F (XPF) protein and functions as an endonuclease producing a 5' single strand cut of 20 nucleotides from the lesion (Figure 7). Early reports suggested that ERCC1 mRNA levels, and not XPF, were correlated with DNA repair capacity when exposed to UV light, suggesting that ERRC1 might be rate-limiting (Bohanes *et al*, 2011; Vogel *et al,* 2000). Those data suggest the hypothesis that *ERCC1* gene expression might be used as a predictive marker for DNA repair capacity, and thus predict platinum compounds cytotoxicity. ERCC1 gene localized on chromosome 19q13.32 and encodes a 32 kDa protein located in the nucleus.

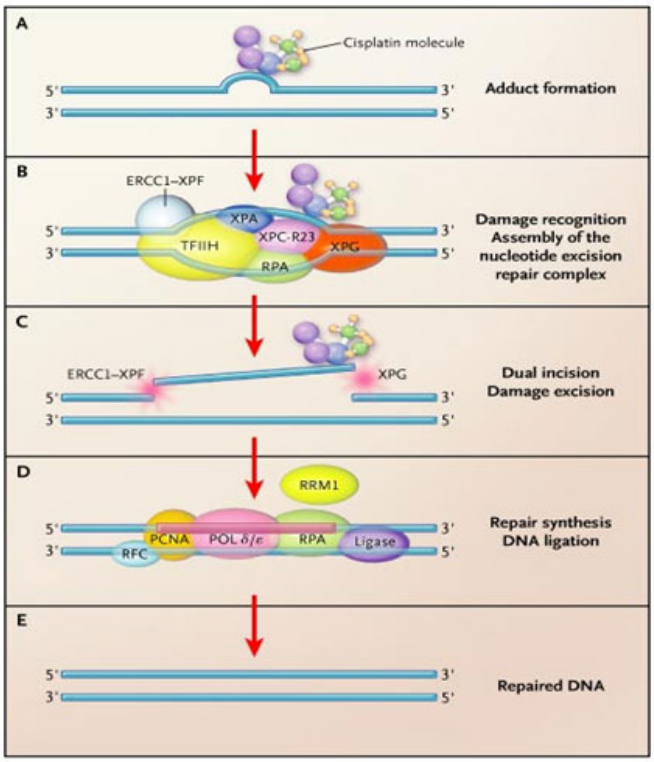

Figure 7 ***Simplified model of genome Nucleotide Excision Repair (NER) system.***

1.10.2 **Thymidylate synthase (TS)**

Thymidylate synthase (TS) is a key enzyme in the *de novo* synthesis of DNA. The reaction catalyzed by TS is the methylation of dUMP, through the transfer of the methyl group provided by the cofactor methylenetetrahydrofolate (CH_2THF) dUMP is converted into deoxythymidine-5′-monophosphate (dTMP). Subsequently, dTMP is phosphorylate by two successive steps to 2'-deoxythymidine-5'-triphosphate (dTTP) an essential precursor for DNA synthesis. TS is target for chemotherapeutic agents because of its central role in DNA synthesis, and it is also of interest because of its rich mechanistic features. Pemetrexed and 5-fluorouracil are the main antitumour agents targeted to the TS (Figure 8). The gene encoding TS is localized on chromosome 18p11.32, the protein consists of 313 amino acids and has a ubiquitous localisation in the cell, i.e. in the nucleus, in the cytoplasm and in the mitochondrion inner membrane and matrix.

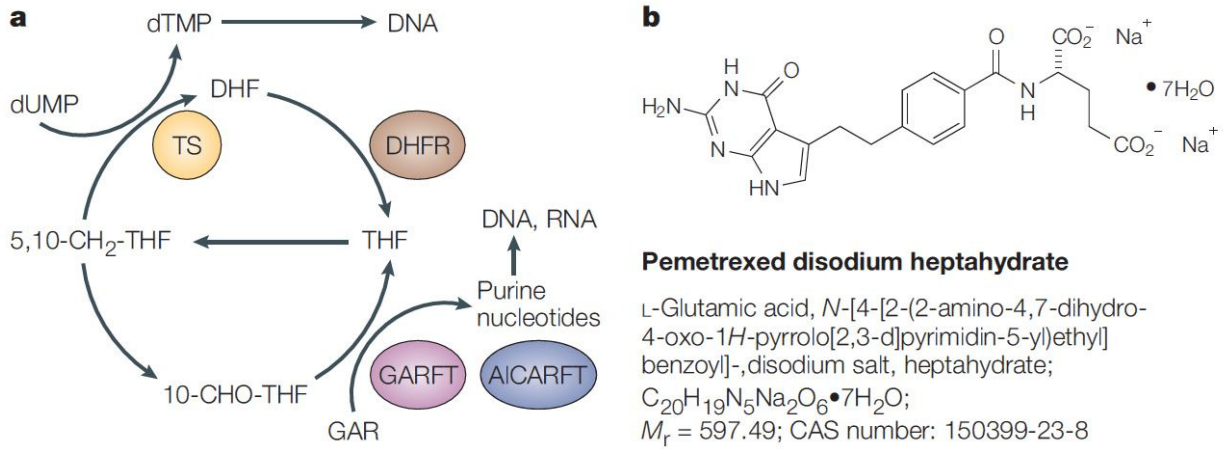

Figure 8 ***a) Simplified illustration of some key enzymatic reactions of folate metabolism, showing enzymes affected by pemetrexed, or its polyglutamates. b) Structure of pemetrexed disodium. AICARFT: aminoimidazole carboxamide ribonucleotide formyltransferase; DHFR: dihydrofolate reductase; GARFT: glycinamide ribonucleotide formyltransferase; THF: tetrahydrofolate, TS: thymidylate synthase.***

1.11 Clonality analysis

In spite of a number of different approaches that have been shortly described above, malignant mesothelioma is not yet to be cured. Understanding more about the initiation of the tumor development and the factors that trigger it is crucial to have the best way to treat or even prevent this cancer. Given the fact that a cell population could be a mixture of slightly different cells, any single method for the treatment may include the chance of the failure, because of the differences of drug sensitivity of the single cells. The most common method to investigate whether a tumour population is homogenous or not is to determine its clonal origin. This approach explores the nature of tumour initiation and categorizes the tumour as mono- or poly-clonal. A clonal population of tumour cells is defined as those cells arising from the mitotic division of a single somatic cell (Seeker-Walker *et al*, 1985), while a polyclonal tumor is known to be initiated by division of multiple differentiated cells. Categorization of a cell population as mono- or polyclonal is made possible by the determination of the inactivated X chromosome of the cells in a given population. The natural event of X chromosome inactivation occurs in all female cells during the early embryogenesis and provides a sufficient tool for tracking a population to their ancestral stage, because once it is determined, the same X chromosome is kept inactivated during the mitosis of the same cell.

1.11.1 X Chromosome inactivation

In females inactivation of one X chromosome occurs in each somatic cell in early embryonic development and is passed onto the progeny of the cell in a stable fashion (Lyonization) (Martin *et a*l, 1978; Lyon *et al*, 1988, Lyon, 1961). Females heterozygous for polymorphic X-chromosome genes are therefore mosaics with respect to X-chromosome activity (Figure 9). In 1961, Mary Lyon proposed that the Barr body, a unique cytological entity situated near the nucleolus that distinguishes female from male cells, was the condensed, inactive female X chromosome. She proposed random X-chromosome inactivation (XCI) as an explanation for this cytological entity. The Lyon hypothesis suggested that one of the two X chromosomes is entirely silenced or inactivated at random in the soma to balance the X-linked gene dosage between XX females and XY males. Her hypothesis was based on the observations of X-linked coat color mutations in heterozygous female mice. In these mice, the phenotype was always a mosaic, consisting of patches of normal or mutant color, rather than a homogenous blending, suggesting that early in development, in the pigmented cells either one or the other X chromosome was inactivated. Thus, if the X chromosome carrying the mutant allele was inactivated, the patch was of normal color, whereas if the X chromosome carrying the normal allele was inactivated, the patch was of mutant color. Beutler and colleagues formulated the XCI hypothesis using studies of the human X chromosome glucose 6-phosphate dehydrogenase (G6PD) gene (Beutler *et al*, 1962). They found that, in females, G6PD activity was not twice as much that of males, as expected by the presence of two X chromosomes, and postulated a dosage compensation mechanism. In females heterozygous for G6PD deficiency, dosage compensation results in G6PD expression at half the rate of normal hemizygous males. This could be attributable to either half-level activity in all cells or normal expression in some cells and low expression in other cells, resulting in overall half-level expression. Using a mixture of male cells with deficient G6PD activity and normal G6PD activity, Beutler and colleagues measured G6PD activity (by glutathione stability) and compared it with the response of female erythrocytes. They found that the response curves of the 2 samples were similar in shape and concluded that intermediate activity in females was probably attributable to the same mechanism as in the mixture of male normal and G6PD activity-deficient erythrocytes. There is evidence that X-chromosome inactivation is related to differential methylation of cytosine in the DNA of X-chromosome genes (Holliday R, 1987).

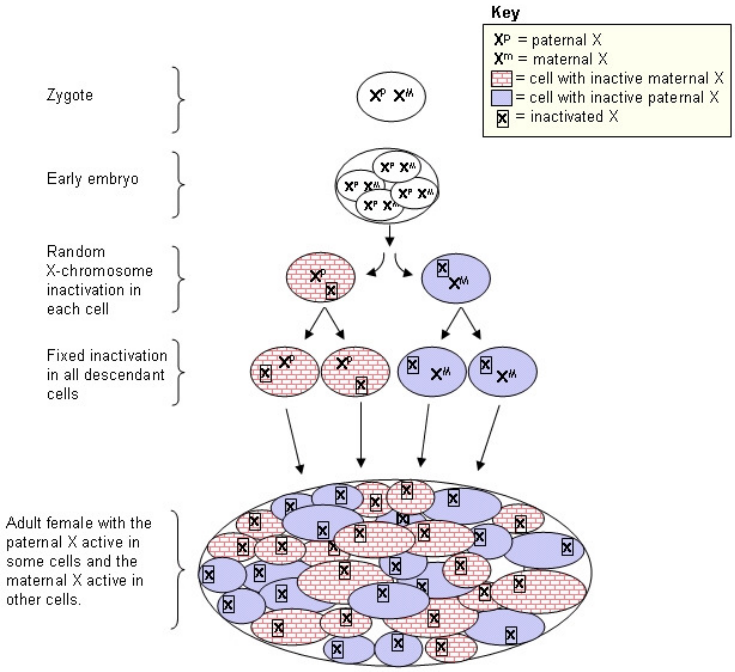

Figure 9 ***X chromosome inactivation Xp: clonal cell with active paternal X chromosome Xm: clonal cell with active maternal X chromosome***

1.11.2 Mechanisms of X-chromosome inactivation

The exact molecular mechanisms underlying XCI are still not fully clarified, but involve several steps, including the determination of the number of X chromosomes per cell, selection of either the paternal or maternal X chromosome for subsequent inactivation, and initiation of the actual inactivating process. It has been demonstrated in mice that there are 3 non coding loci, located near the center of inactivation of X chromosome that play a pivotal role in the mechanism of X-chromosome inactivation. These loci are: non coding RNA X (inactive)-specific transcript (Xist), its antisense partner Tsix, and the intergenic locus Xite. Xist is necessary for cis inactivation of the X chromosome. In vitro, Xist is able to silence also the autosomal surrounding chromatin in case of X: autosome translocation, but in an incomplete manner, due to instability of autosome inactivation (Lee J.T *et al*, 1999). Tsix and Xite work in parallel to Xist by maintaining X-chromosome transcriptional competence (Ogawa *et al,* 2003). Although the functions of these 3 loci have been deduced using complementary cell lines, the actual physical interactions of these components are less well known. Xist is proposed to achieve cis-inactivation of the X chromosome through close interactions between its RNA transcript and the segment of X chromosome to be inactivated (Penny G.D. *et al*, 1996). The putative trans-interactions, based on the need to determine one X to be exclusively activated and the other X to be exclusively inactivated, remained elusive, until the recent demonstration that the 2 X chromosomes undergo inter-chromosomal pairing (Heard E.,

2004). It is remarkable that inter-chromosomal pairings typically occur in germ cells undergoing meiosis, rather than in somatic cells undergoing mitosis. X-chromosome inactivation timing is crucial to the interpretation of X chromosome inactivation pattern (XCIP)-based clonality assays. It has been assumed that pre-blastocyst embryos express both X chromosomes and that inactivation did not occur until after implantation and the embryonic stem cells began to differentiate into separate cell lineages (Okamoto *et al,* 2004). Recent experiments, however, demonstrate that XCI occurs as early as the 4-cell stage of the embryo, but is variable and leaky and does not become stabilized until after implantation, but before differentiation of embryonic stem cells into the various cell lineages (Huynh *et a*l, 2003). XCI before cell lineage differentiation is crucial for the interpretation of XCIP clonality studies. Hematopoietic cell lines derive not from a single embryonic stem cell but from several progenitors, allowing for the mosaic expression of genes from both X chromosomes (Prchal *et al*, 1996).

2 AIMS OF THE STUDY

1) Given to only a few low-powered studies have investigated the presence and frequency of EGFR gene mutations in malignant pleural mesothelioma (Cortese *et al*, 2006; Enomoto *et al*, 2012), and none has searched for mutations in the KRAS, BRAF and PI3KCA downstream effectors, in this study we searched a large series of histological MPM samples for mutations in EGFR gene and its main downstream signaling effectors in order to evaluate their frequency and possible prognostic significance, and their possible use as predictors of the response of MPMs to targeted therapies.

2) The golden standard in the treatment of patients with malignant mesothelioma is the multimodal administration of platinum and pemetrexed. Currently there are not biomarkers which predict the clinical outcome and the prognosis for this tumour. The second aim of this work was to retrospectively investigate in a series of MPM patients, randomly treated with platinum and pemetrexed (alone and in combination), ERCC1 and TS gene and protein expression to determine whether they can provide informations about the clinical outcome and/or can have a prognostic value.

3) Identifying whether a tumor is monoclonal or polyclonal at start, have critical implications in terms of early therapeutic intervention. The third aim of the study was to evaluate the clonality pattern of malignant mesothelioma.

3 MATERIALS AND METHODS

In this study we used two different clusters of MPM tumour samples: in the first case we collected the samples from the Thoracic Unit of the University Hospital of Novara on which we performed the sequencing analysis of EGFR and downstream pathways and the evaluation of ERCC1 and TS protein and gene expression (Novara samples).
In the second case the tumour samples we used to evaluate the clonality assessment of malignant mesothelioma were obtained from Dr. H. I. Pass (NYU, New York) and from Dr.Paul Sugarbaker (WCI, Washington, DC) in accordance with protocols approved by the Institutional Review Board of each center and upon patients informed consent (US samples).

3.1 Novara samples

3.1.1 Samples collection and preparation

In this study we involved a large number of MPM patients admitted to the Thoracic Unit of the University Hospital of Novara between January 2008 and March 2013, all of whom were diagnosed as having MPM on the basis of multiple pleural biopsies taken by means of video-assisted thoracoscopy. The tumour samples were immediately fixed in formalin for 24 h, embedded in paraffin, and routinely processed for histology and immunohistochemistry. The diagnosis of MPM was based on standard histological and immunohistochemical criteria, including positivity to calretinin, vimentin, and cytokeratins 5 and 6, and negativity to carcinoembryonic antigen, thyroid transcription factor 1, and Ber Epy 4. From the analysis of the clinical records we obtained the following data:

- Personal data of the patient
- MPM diagnosis date
- Surgery or biopsy date
- Treatment
- Status (Dead/Alive)
- Follow up: from the date of diagnosis to June 2013 for alive patients, and from the date of diagnosis to the date of death for dead patients.

The MPMs were classified on the basis of the WHO classification of pleural tumours (Travis et al, 2004), and clinically and pathologically staged on the basis of the TNM staging system (Sobin et al, 2009).Looking through the WINANA database of the Pathology Department of "Maggiore della Carità" Hospital we got these data (snomed # M-90523):

- haematoxylin/eosin-stained slides of the pleural biopsies and corresponding formalin-fixed, paraffin-embedded blocks
- histotype: epithelioid, sarcomatoid and biphasic.

An expert pathologist review the haematoxylin/eosin-stained slides of each case to:

- confirm the diagnosis and the histotype;
- to select the area with 70% of tumour cells (minimum required for the sequencing analysis and gene expression evaluation);
- identify the best sample, in term of cellularity, in case we have more than one biosy or surgery piece.

The tumoral areas of the formalin-fixed paraffin-embedded sections were macro-dissected manually, and then five 5 µm thick sections were prepared and collected in a 1.5 mL tube in order to perform the DNA and RNA extraction. 3 µm thick sections were cutted to perform immunohistochemistry staining.

3.1.2 DNA extraction

Genomic DNA was extracted using 450 µl of EDTA-SDS/proteinase K (SDS 1%, EDTA 20mM, Tris HCl pH 7,5 20mM) followed by phenol-chloroform, and resuspended with 30 µL of DEPC-treated and RNAse free water (Promega, Madison, USA). We include a negative control of extraction every 5 samples. The DNA concentration was evaluated by reading the absorabance at 260nm by mean of a spectrophotometer (Eppendorf, Amburgo, Germania), moreover to assess the purity of DNA we measure the ratio 260/280 and 260/230.

3.1.3 Mutational analysis

EGFR gene

All of the samples were analysed using the TheraScreen EGFR29 Mutation Kit (QIAGEN, Manchester, UK), which combines the two technologies of ARMS and Scorpion chemistry in order to detect mutations in a real-time polymerase chain reaction (PCR). This kit allows the detection of in-frame deletions on exon 19, insertions on exon 20, and G719X, S768I, T790M, L858R and L861Q mutations against a background of WT genomic DNA with a sensitivity of 1%. PCR plate and reaction mix were performed according to the manufacturer's instructions, with 50 ng of DNA for each well. DNA amplification was performed with the following cycles: denaturation at 95°C for 4 min, 40 cycles of 95°C for 30 sec and 60°C for 1 min. Negative and positive controls were used in every reaction plate, moreover the kit contains a control reaction mix that amplify exon 2 of *EGFR* to evaluate amplifiable DNA in the tested samples. Results interpretation was done following the datasheet instruction: sample quantification cycle must be within the range of 21.92 and 37.00. Sample was classified as positive when both control and mutation curves were positive according to the above limits. In order to determine the presence of other less common mutations, the samples underwent further PCRs in order to amplify the whole sequence of exons 18-21 of the EGFR gene. PCR conditions primers and are shown in Table 1.

KRAS gene

The KRAS gene was analysed by means of a mutant-enriched PCR (ME-PCR) in order to detect the hotspots in codons 12 and 13 of exon 2 that include more than 95% of the known gene mutations. The ME-PCR consisted of two amplification steps (semi-nested PCR) in which artificial restriction sites were introduced into the wild-type amplicon using mismatched primers. The restriction sites (BstNI for codon 12 and BglI for codon 13) introduced during the first PCR step were localised immediately next to the KRAS codon in the analysis in order to distinguish wild-type and mutant sequences. The wild-type amplicons were then digested by restriction enzymes and the mutant products were enriched for a second round of amplification. Each round of amplification was followed by overnight digestion with BstNI and BglI restriction enzymes(10 U/ml); respectively for codon 12 we digested with BstNI at 60°C and for codon 13 with BglI at 37°C in a 20 µl reaction volume. Products of PCR amplification were analyzed by gel electrophoresis on 3% agarose gel containing Ethidium Bromide (10ug/ml), and resolved DNA bands were visualized on a UV transilluminator (MarcoVe UV-20, Hoefer). ME-PCR has a sensitivity of up to 0.01%. All of the

samples were underwent automated sequencing by using an ABI PRISM 3130 (Applied Biosystems, Foster City; CA, USA) and reverse primers.

BRAF gene

Exon 15 of the BRAF gene (which contains the hotspot codon 600, where more than 90% of gene mutations occur) was analysed by means of direct sequencing after PCR reaction starting from 50 ng of genomic DNA. The primers and PCR conditions are shown in *Table 1*.

PI3KCA gene

The analysis of the PIK3CA gene was concentrated on exons 9 and 20, which include all of the hotspot codons, the primers and PCR conditions are shown in *Table 1*. The mutational status of PIK3CA was then investigated by means of direct sequencing.

Sequence analysis

All of the PCR products and KRAS second enzymatic digestions were analysed by means of 3% agarose gel electrophoresis, and then purified using NucleoSpin Gel and the PCR clean-up kit (Macherey-Nagel, Düren, Germany). The sequence of each gene was analysed using an ABIPrism 3130 Genetic Analyzer (Applied Biosystems, Foster City, CA, USA), and all of the mutated cases were confirmed twice starting from independent PCR reactions.

Gene	Primer name	Sequence	Cycle	Length
KRAS codon 12 (outer)	3F 10B	5′-ACTGAATATAAACTTGTGGTAGTTGGACCT–3′ 5′-ACTCATGAAAATGGTCAGAGAAACCTTTAT-3′	95 °C × 10 min; (95 °C × 30 s, 50 °C × 1 min, 72 °C × 1 min) × 20 cycles; 72 °C × 3 min	143
KRAS codon 13 (outer)	9F 10B	5′-ACTGAATATAAACTTGTGGTAGTTGGCCCTGGT-3′ 5′-ACTCATGAAAATGGTCAGAGAAACCTTTAT-3′	95 °C × 10 min; (95 °C × 30 s, 54 °C × 1 min, 72 °C × 1 min) × 20 cycles; 72 °C × 3 min	113
KRAS codon 12 (inner)	3F 14B	5′-ACTGAATATAAACTTGTGGTAGTTGGACCT-3′ 5′-TCAAAGAATGGTCCTGGACC-3′	95 °C × 10 min; (95 °C × 30 s, 54 °C × 1 min, 72 °C × 1 min) × 45 cycles; 72 °C × 3 min	143
KRAS codon 13 (inner)	9F 4B	5′-ACTGAATATAAACTTGTGGTAGTTGGCCCTGGT-3′ 5′-TCAAAGAATGGTCCTGCACC-3′		113
EGFR exon 18	EGFR18F EGFR18R	5′-TCCAGCATGGTGAGGGCTGAG-3′ 5′-GGCTCCCCACCAGACCATG-3′	50 °C × 2 min; 95 °C × 10 min; (95 °C × 40 s, 58 °C × 40 s, 72 °C × 35 s) × 40 cycles; 72 °C × 3 min	242
EGFR exon 19	EGFR19F EGFR19R	5′-TGGGCAGCATGTGGCACCATC-3′ 5′-AGGTGGGCCTGAGGTTCAG-3′		217
EGFR exon 20	EGFR20F EGFR20R	5′-CCTCCTTCTGGCCACCATGCG-3′ 5′-CATGTGAGGATCCTGGCTCC-3′		296
EGFR exon 21	EGFR21F EGFR21R	5′-CCTCACAGCAGGGTCTTCTC-3′ 5′-CCTGGTGTCAGGAAAATGCT-3′		229
BRAF exon 15	BRAF15F BRAF15R	5′-TCATAATGCTTGCTCTGATAGGA-3′ 5′-GGCCAAAAATTTAATCAGTGGA-3′	95°C × 10 min; (95 °C × 15 s, 52 °C × 30 s, 72 °C × 30 s) × 45 cycles; 72 °C × 3 min	224
PIK3CA exon 9	PIK3CA9F PIK3CA9R	5′-GGGAAAAATATGACAAAGAAAGC-3′ 5′-CTGAGATCAGCCAAATTCAGTT-3′	95 °C × 10 min; (95 °C × 35 s, 56 °C × 30 s, 72 °C × 30 s) × 40 cycles; 72 °C × 10 min	251
PIK3CA exon 20	PIK3CA20F PIK3CA20R	5′-CTCAATGATGCTTGGCTCTG-3′ 5′-TGGAATCCAGAGTGAGCTTTC-3′		241

Table 1 Forward and reverse primers, PCR conditions and amplicon length of KRAS, EGFR, BRAF and PI3KCA exons investigated.

3.1.4 Protein and gene expression analysis.

mRNA extraction and reverse transcription.

RNAs were isolated from paraffin-embedded MPM tumor samples verified by an expert pathologist to contain at least 50% of tumor cells. After deparaffinization with xylene, RNA was isolated by the RecoverAll Total Nucleic Acid Isolation Kit (Ambion, Applied Biosystems) following the datasheet instruction and resuspended in 60 µl of elution solution. RNA yields were checked by reading the absorabance at 260nm by mean of a spectrophotometer (Eppendorf, Amburgo, Germania). 500 ng sample of total mRNA was reverse transcribed to cDNA using RevertAid First Strand cDNA synthesis kit (Fermentas, St. Leon-Rot, Germany) using 0,2 µg/µL of random examers.

Quantitative Real-time PCR.

Quantitative real-time polymerase chain reaction (qRT-PCR) was performed in triplicate with 3µl of cDNA, 1X of TaqMAn Universal PCR Master Mix no AmpErase UNG, 1X of premade TaqMan Gene Expression Assay (Assay ID: *ERCC1:* Hs01012161_m1; *TS:*Hs00426586_m1Applied

Biosystems) in a final reaction volume of 20 µl. Samples were amplified by the ABI 7500 real-time PCR machine (Applied Biosystems) under the following thermal profile: an initial incubation at 95°C for 20 seconds, 40 cycles of denaturation at 95°C for 15 seconds followed by annealing and extension at 60°C for 30 seconds. Assay results were normalized to 18S rRNA (Eukaryotic 18S rRNA Endogenous Control; Applied Biosystems) and gene expression quantification was performed by ΔΔCT methods using Sequenze Detector System 7500 software v 2.0.4. We used as a calibrator a pool of normal tissues including lung, liver, colon and pleura.

Immunohistochemistry

Immunohistochemistry was performed on 3-µm thick tissue sections by using anti-ERCC1 (clone 8F1, dilution 1:100; ThermoScientific, Erembodegem, Belgium) and anti-TS (clone TS106, dilution 1:50; Dako, Glostrup, Denmark) monoclonal antibodies. ERCC1 immuno reaction was performed on Ventana BENCHMARK® XT instrument using UltraView DAB kit (Ventana Medical Systems, Tucson, USA), whereas DAKO Autostainer (Dako, Glostrup, Denmark) was used for TS immunostaining. For epitope retrieval, slides were exposed on heat EDTA, then, endogenous peroxidase activity was blocked by incubation with H_2O_2 3% (ERCC1: 30 min EDTA and 4 min H_2O_2– TS: 14 min EDTA and 10 min H_2O_2). ERCC1 primary antibody incubation was carried out for 32 minutes at 37°C while anti-TS incubation was performed for 60 minutes at room temperature. The reaction was revealed with EnVision HRP Rabbit/mouse detection system (DakoCytomation, Denmark), using 3' 3-diaminobenzidine (Dako) as chromogen. Negative controls were obtained omitting the primary antibody. Proliferating germinal center lymphocytes of a reactive lymph node and normal mesothelial cells adiacent the tumor served as positive controls for TS and ERCC1, respectively. (Olaussen KA *et al*. 2006; Zucali AP *et al*., 2011). The slides were counterstained with hematoxylin, dehydrated, and mounted.

Immunohistochemistry evaluation.

The sections were reviewed and scored by a pathologist that was blinded to patient identity and clinical outcome. In agreement with previous studies (Olaussen *et al*, 2006), the results were interpreted by a system on the basis of staining intensity and the number of stained cells. Staining for ERCC1 was considered positive when tumor cells showed nuclear reactivity, while TS positivity was on the basis of both nuclear and cytoplasmic reactivity. The percentage of positive tumor cells and the staining intensity were analyzed by a semiquantitative histologic score (H-score). In particular, the staining intensity of tumor—ranging from low (score 1) to moderate and

high scores (2 and 3)—was multiplied by the percentage of positive neoplastic cells, in detail: 0 if 0%, 0,1 if 1% to 9%, 0,5 if 10% to 49%, and 1,0 if 50% or more, thus obtaining values from 0 to 3.

3.1.5 Statistical analysis.

Mutational data analysis.

The associations between categorical variables were determined using the chi-squared or Fisher's exact test. The statistical differences of the average values were tested using a Student's t test and analysis of variance followed by Bonferroni's test. The impact of the different variables on long-term outcomes was analysed using the Kaplan-Meier method of analysing disease specific survival (DSS); the survival data were compared using the log-rank test. P values of <0.05, with a 95% confidence interval, were considered statistically significant

Biomarkers data analysis.

Patient characteristics were described in terms of number and percentage, median and range. DSS was calculated from the time of diagnosis to the time of death (caused by the specific disease). DSS was evaluated with the Kaplan–Meier method and groups were compared with the Log-rank. The association between mRNA or H-score and the clinical-pathological features of the patients was analised respectively by the mean of Kruskal Wallis test and Fisher's Exact test. The correlation between TS and ERCC1 gene expression was analised by the Pearson's test, whereas the correlative analysis between TS and ERCC1 protein expression was carried out by the Kendall test. All the statistical analyses were performed using the R software. The level of significance was set at P=.05.

3.2 US samples

US tumour samples derived from MPM female patients who underwent surgery; they were collected at the following institutions: Department of Cardiothoracic Surgery, New York University, New York, NY; MedStar Washington Hospital Center, Washington, DC; University of Wisconsin School of Medicine and Public Health Department of Surgery, Madison, WI, and at the Department of Surgery, Penn Presbyterian Medical Center, Philadelphia, PA, in accordance with protocols approved by the Institutional Review Board of each center and upon patients informed consent. Human specimens tissues were collected during surgical tumour resection, immediately frozen and processed for laser microdissection and DNA extraction. The identification of tumor and normal

tissues in each sample was performed by hematoxylin-eosin (H&E) staining.

3.2.1 HUMARA Assay

Tumors and normal tissues were dissected by Laser Capture Microdissection using a MMI CellCut Plus (Molecular Machines & Industries, MI, USA). LCM tubes were incubated for 48 hours at 37°C, centrifuged, and subjected to protein digestion for two additional days at 55°C, by adding fresh Proteinase K daily. DNA was extracted by using DNeasy Blood&Tissue Kit (Qiagen, Valencine, CA) (Figure 10). DNAs were then digested with HpaII enzyme: 100 ng of either tumor or normal DNA were digested with 10 U Hpa II restriction enzyme (New England Biolabs, Ipswich, MA, USA) at 37ºC overnight in a 20 µl reaction volume. Separate aliquots of DNA were subjected to mock digestion without the enzyme. After incubation, the restriction enzyme was inactivated at 65ºC for 20 min. HpaII-digested or mock-digested DNA was then subjected to PCR reaction, using the following primers: 5 FAM-labeled forward primer, 5'ACC GAG GAG CTT TCC AGA AT3'; reverse primer, 5'TGG GGA GAA CCA TCC TCA C3'. Thermal cycling conditions included the following steps: denaturation at 95°C for 10 minutes; 30 cycles at 95°C for 30 seconds, 55°C for 30 seconds, and 72°C for 30 seconds; and a final extension at 72°C for 10 minutes. Products of PCR amplification were analyzed by gel and capillary electrophoresis. Gel electrophoresis was performed on 3% agarose gel containing ethidium bromide (10ug/ml), and resolved DNA bands were visualized on a UV transilluminator (Biorad). For capillary electrophoresis, PCR products were mixed with 95% formamide and loading buffer (5% blue dextran, 25 mM EDTA) containing Rox-500. The mixture was then loaded on a 5% Long Ranger–6 M urea gel in TBE buffer. Electrophoresis was performed at 200 W for 2.25 hours, and the data were analyzed by an on a ABI 3100 Genetic Analyzer (Applied Biosystems, Foster City, CA) and quantified by Genescan 3.1 software (Applied Biosystems) (Figure 11). We used DNA extracted from female melanoma cell line (labelled #1290) as a monoclonal control and DNA obtained from a healthy female blood sample (labelled L-IV-II) as a polyclonal control.

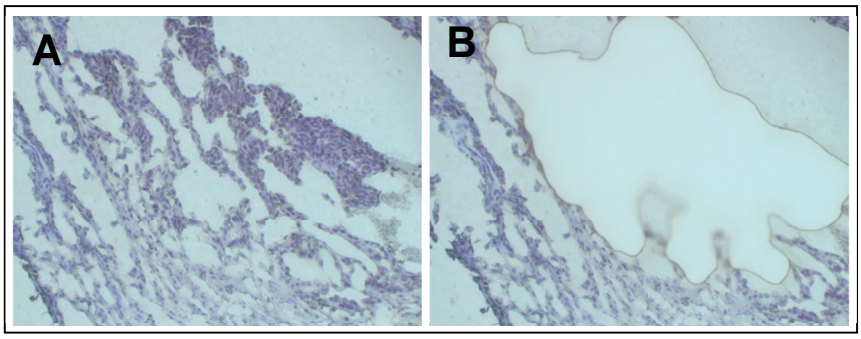

Figure 10 Laser capture microdissection of MM. H&E of a representative MM tumor section is shown before a) and after b) tumor tissue was collected by laser capture microdissection.

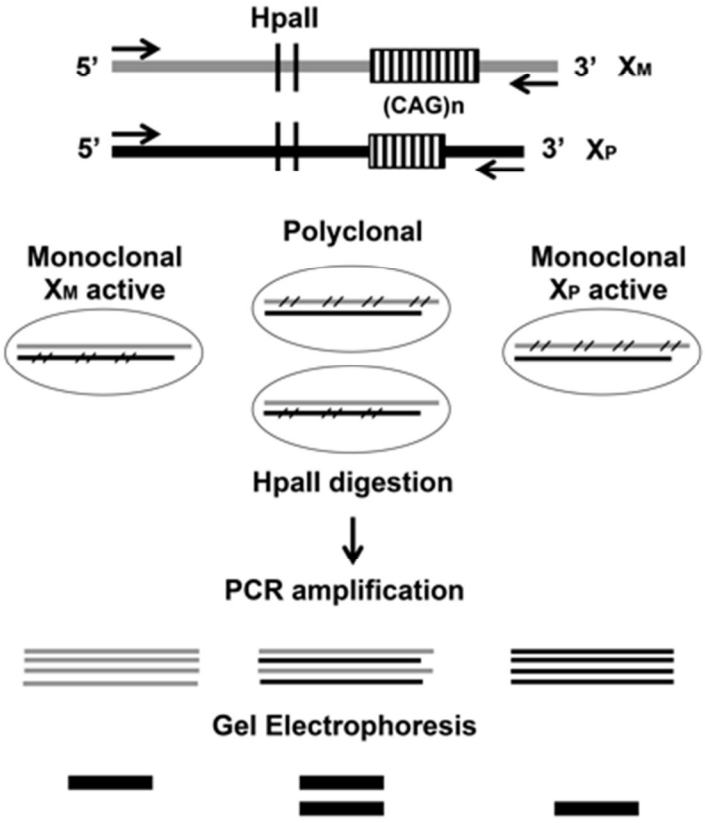

Figure 11 Schematic diagram of the HUMARA assay. *Maternal and paternal X chromosomes carry different numbers of CAG repeats at the Humara locus. HpaII methylation sensitive sites are located at the polymorphic CAG region. During embriogenesis, random X chromosome inactivation occurs in female individuals, resulting in methylation of either the paternal or maternal X chromosome in different cells. Therefore, monoclonal cell population, derived from the division of a single ancestor cell, shares the same inactivated X chromosome, while a polyclonal population, derived from more than one ancestor cell, contain both cells with either inactive maternal or paternal X chromosome. HpaII digestion removes the unmethylated alleles, allowing amplification of the methylated HUMARA locus. Electrophoresis of the PCR products will resolve respectively in a single band or two bands of different size. Arrows indicate the primer sites, HpaII denotes the methylation sensitive endonuclease sites; arrows indicate primer annealing regions. Cross bars indicate the methylated chromosome.*

3.2.2 Data Analysis

For each sample, the allele intensities were measured as the peak areas of both alleles, which is proportional to the molar amount of DNA. The allele ratios were first calculated by dividing the ratio (RU=A1U/A2U) of the non-HpaII digested sample, by the ratio (RD=A1D/A2D). The AR calculation (AR=RU/RD) corrects for any preferential amplification of one allele that might occur if the alleles are different in length. The clonality ratio is then calculated by dividing the AR of the tumor DNA by the AR calculated for the normal tissue (CR=ART÷ARN). This final calculation corrects for a potential skewed lyonization. A CR $\geq$ 3.0 or $\leq$ 0.3, representing a preferential loss of intensity in the digested sample of one of the two alleles present in the tumor sample, was scored as a monoclonal pattern.

4 RESULTS

4.1 Mutational analysis of EGFR and downstream pathways

4.1.1 Clinical Features

Out of 77 MPM patients studied, 57 were male (74%) and 20 were female (26%); their average age at the time of diagnosis was 68 years (range 43–90, median 64.5 years). Of these, 50 patients (64.9%) had previously been exposed to asbestos at work. Histological examination showed that 59 MPMs (77%) were epithelioid, 10 (13%) biphasic, and 8 (10.4%) sarcomatoid. In total, 41 patients had stage II tumours, 30 stage III tumours, and 6 stage IV tumours. Eastern Cooperative Oncology Group PS was 0–2 in 68 patients, and 42 in nine patients. In all, 41 patients were treated with platinum plus pemetrexed (Alimta) and 22 with platinum alone; 14 received no treatment because their performance status (PS) was 42 or because they refused. For this work we stopped the follow-up (FU) at June 2012, at this date we collected FU data from 74 patients (three were lost to follow-up). In all, 15 patients were still alive at June 2012 with a median FU of 24.5 months (range 14–39 months). The median disease specific survival (DSS) of the cohort as a whole was 12.5 months (range 1–39 months) (*Table 2*).

4.1.2 Mutational Analysis

EGFR gene mutational profiling.

No mutations were detected in the EGFR gene by direct sequencing or the Scorpions-ARMS assay, even though the latter has a sensitivity of 1% (vs the10–20% of direct sequencing).

KRAS and BRAF gene mutational profiling.

KRAS gene was successfully amplified in all of the samples, five of which showed mutations: two patients had the GGT-G*t*T point mutation in codon 12 leading to a glycine-to-valine amino-acid substitution (G12V); two had the GGC-G*a*C point mutation in codon 13 leading to a glycine-to aspartic acid substitution (G13D); and one had the rare GGC-*a*GC mutation in codon 13 leading to a glycine-to-serine substitution (G13S). Three of the five mutations occurred in patients with epithelioid MPMs (G12V, G13D, and G13S), one in a patient with a biphasic MPM (G13D), and one in a patient with a sarcomatoid subtype (G12V) (Table 2). All five patients with KRAS

mutations reported previous occupational asbestos exposure. The BRAF gene mutational analysis showed the classical valine to-glutamic amino-acid substitution in codon 600 (V600E) in three patients: two with epithelioid MPMs and one with a biphasic tumour (Table 2). None of them reported previous occupational asbestos exposure.

PI3KCA gene mutational profiling.

The DNA of exons 9 and 20 of the PIK3CA gene was successfully amplified from 75 of the 77 specimens. A point mutation was detected in only one case: it occurred in exon 20, and led to a methionine to isoleucine substitution in position 1040 (M1040I). The patient had a biphasic mesothelioma and no previous occupational asbestos exposure (*Table 2*).

Patient	Gene	Amino-acid substitution	Gender	Age	Histotype	Asbestos exposure	DSS
1	***KRAS***	G12V	Male	81	Sarcomatoid	Yes	4
2		G12V	Male	55	Epithelioid	Yes	14
3		G13D	Male	82	Epithelioid	Yes	4
4		G13S	Male	60	Epithelioid	Yes	5
5		G13D	Male	77	Biphasic	Yes	19
6	***BRAF***	V600E	Female	51	Epithelioid	None	9
7		V600E	Male	57	Biphasic	None	19
8		V600E	Male	73	Epithelioid	None	33
9	***PIK3CA***	M1040I	Male	68	Biphasic	None	7

Abbreviation: DSS = disease-specific survival.

Table 2 Mutations in the EGFR downstream pathway were identified in nine patients (12%): five in the KRAS gene, three in the BRAF gene, and one in the PIK3CA gene.

4.1.3 Statistical analysis.

The correlations between the presence/absence of gene mutations and demographic, clinical and pathologic features (gender, age, occupational asbestos exposure, history of previous cancer, histological type, ECOG PS, treatment) were investigated, without finding any significant differences (*Table 3*).

	Wild type ($n = 68$)	Mutations ($n = 9$)	*P*-value
Age, mean ± s.d. (years)	66 ± 21	67 ± 12	0.89
Gender (male proportion)	49/68	8/9	0.491
Previous cancer	5/68	2/9	0.385
Asbestos exposure	44/68	6/9	0.799
Histological subtype			
Epithelial	54/68	5/9	0.241
Biphasic	7/68	3/9	0.135
Sarcomatoid	7/68	1/9	0.623
ECOG score			
0–2	60/68	8/9	0.892
>2	8/68	1/9	0.617
Clinical stage			
II	37/68	4/9	0.689
III–IV	31/68	5/9	0.576
Treatment type			
None	13/68	1/9	0.623
Platinum	19/68	3/9	0.876
Platinum + pemetrexed	36/68	5/9	0.776

Abbreviations: ECOG = Eastern Cooperative Oncology Group; s.d. = standard deviation.

Table 3 Correlations between the presence/absence of gene mutations and demographic, clinical and pathologic features

The Kaplan-Meier analysis of the influence of some variables on long-term outcomes revealed no difference in DSS between the patients with and without gene mutations (P = 0.552). Moreover, separate evaluation of the patients with KRAS and BRAF mutations did not indicate any advantage in terms of DSS (P = 0.363 and P = 0.752) and, within the mutated group, no mutation significantly correlated with DSS (KRAS P = 0.363; BRAF P = 0.187). Interestingly, the patients with KRAS gene mutations reported occupational asbestos exposure, whereas those with BRAF and PI3KCA gene mutations did not. When the DSS of the patients with reported asbestos exposure was considered, the five KRAS gene mutated patients had a worse prognosis than those with wild-type KRAS (n=42), although the difference was not statistically significant (mean survival 9.20 ± 6.91 vs 15.6 ± 10.39 months; P = 0.188). On the contrary, the DSS of the patients without reported occupational asbestos exposure was better in the BRAF gene mutated patients (n=3) than in those without BRAF mutations (n=22) although, once again, the difference was not statistically significant (mean survival 20.33 ± 12.06 vs 12.1 ± 8.37 months; P = 0.140) (Figure 12).

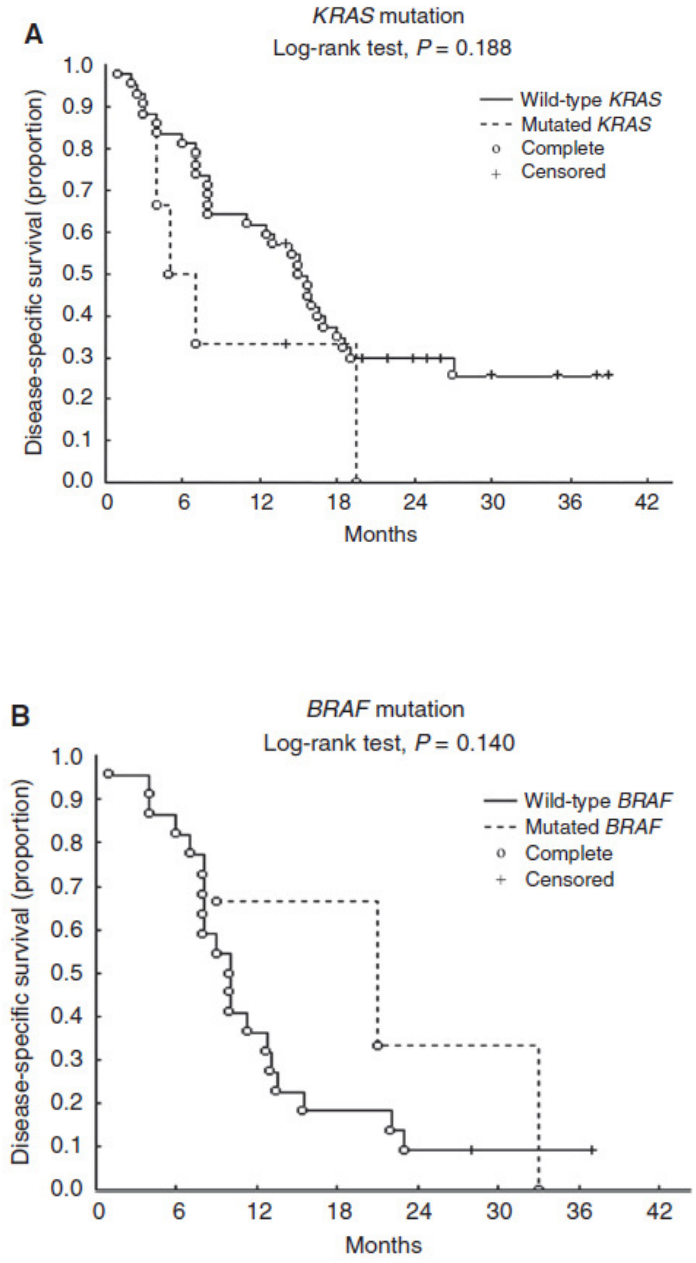

Figure 12 a) Kaplan-Meier DSS curves for MPM patients with KRAS mutation Vs wild-type b) and BRAF mutation Vs wild-type

4.2 Predictive and Prognostic Biomarkers

4.2.1 Clinical features

We collected 148 MPM specimens from patients who underwent pleural biopsy and/or surgical treatment. Out of 148 MPM patients studied, 103 were male (70%) and 45 were female (30%); their average age at the time of diagnosis was 75 years (range 27–90, median 65.3 years). Of these, 77 patients (53%) had an history of occupational asbestos exposure, 65 had not been exposed (44%),

six were lost to asbestos exposure information (3%). Histological examination showed that 108 MPMs (73%) were epithelioid, 20 (13,5%) biphasic, and 20 (13.5%) sarcomatoid. In all, 2 patients received Alimta, 80 patients were treated with platinum plus Alimta and 27 with platinum alone; 31 received no treatment because their performance status (PS) was, because they refused or because advanced tumour, we were not able to collect the treatment information for 8 patients. In this study we involved patients with a follow-up (FU) of at least 12 months and we stopped it at June 2013. At this date we collected disease specific survival (DSS) data from 145 patients (three were lost to follow-up). The median DSS of the cohort as a whole was 12.5 months (range 1–39 months); for alive patients the median DSS was 13 months (average 16,4 months; range 1–39 months) while for dead patients the median DSS was 8 months (average 10,5 months, range 1-39 months).

4.2.2 Survival analysis

We first investigated the correlation between the survival and the MPM histologic subtype: the Kaplan-Meier curves and the statistical analysis carried out with Logrank test showed, as expected, a better prognosis in those patients with epithelioid MPM than in the biphasic and sarcomatoid (P=0.002) (Figure 13) (Montanaro *et al*, 2009). As shown in Figure 14, we analyzed the correlation between DSS and treatment, finding that patients who received platinum plus alimta had a better outcome than the other (Logrank test P=1.49e-08). Moreover we found a statistical correlation between age and DSS (Logrank test P=0.037) (Figure 15).

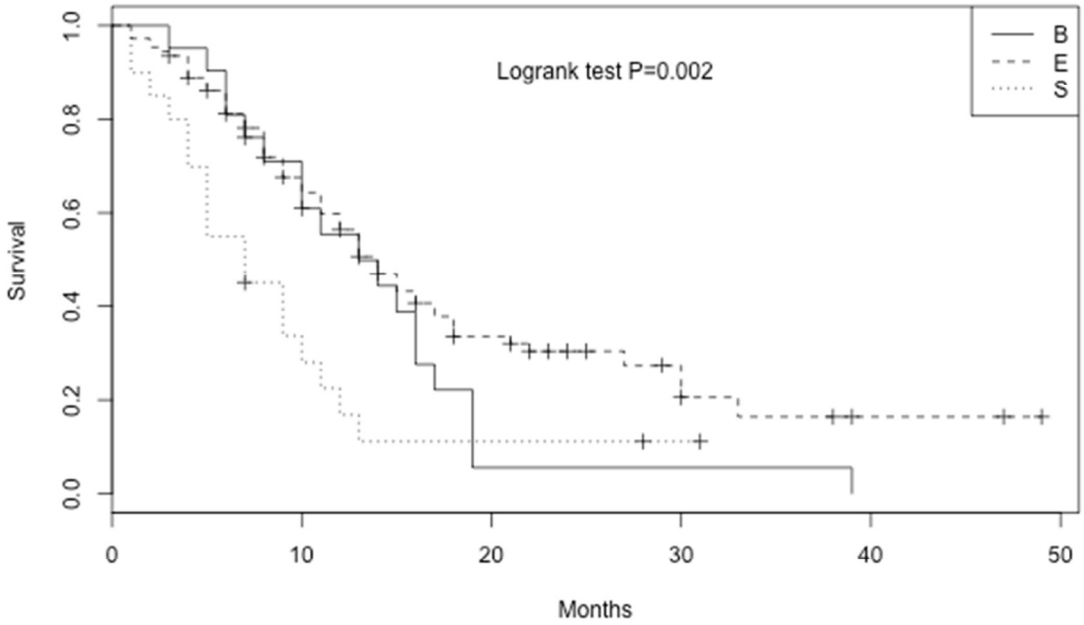

Figure 13 ***Kaplan-Meier analysis in MPM patients with different histotypes. B=biphasic; E=epithelioid; S=sarcomatoid***

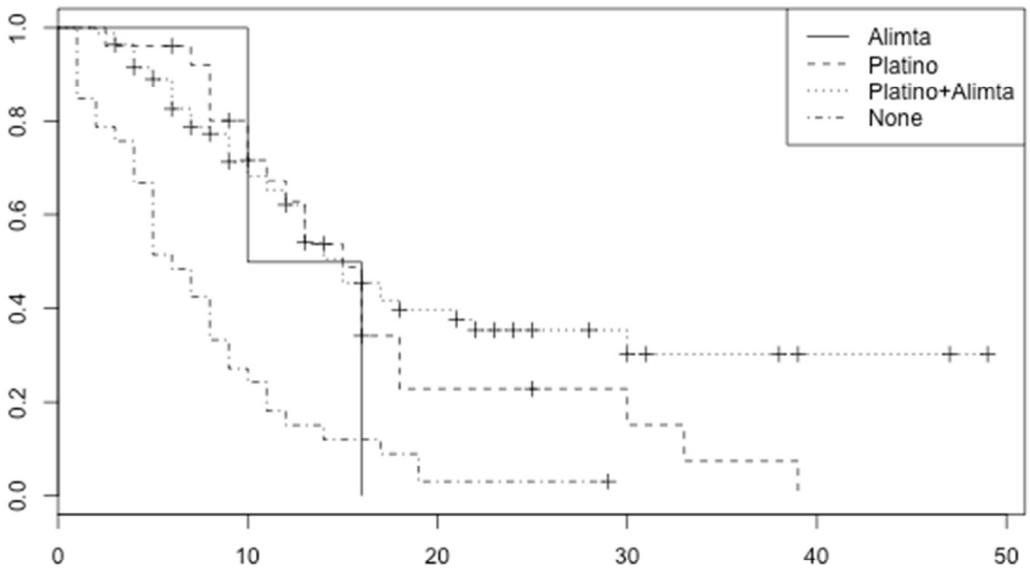

Figure 14 ***Kaplan-Meier analysis in MPM patients who received different therapies.Platinum (solid line); Platinum+Alimta (dashed line); No therapy (dotted line)***

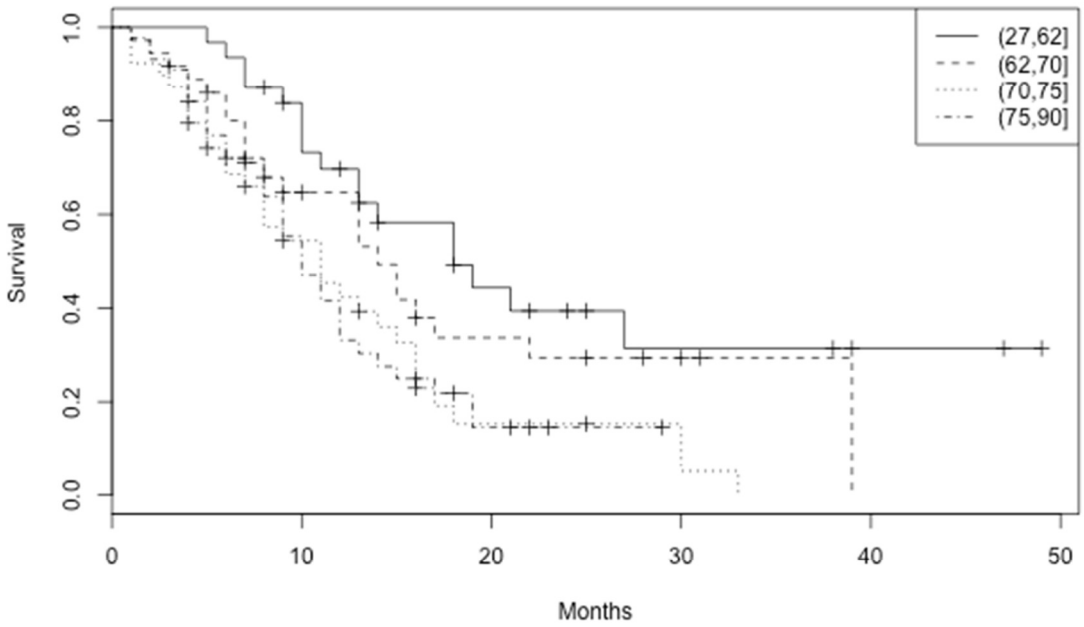

Figure 15Kaplan-Meier analysis in MPM patients divided in different age classes.

4.2.3 ERCC1 Protein expression

ERCC1 immuno-staining was successfully performed in all the 148 cases. The majority of the cases (92/148 - 62%) had H-score 3. Figure 16 shows in detail the distribution of the H-score values: 22 cases had H-score 2 (22/148-14%), 5 cases 1.5 (5/148-3.5%), 13 cases 1 (13/148-9%), 4 cases 0.5 (4/148-3%), 4 cases 0.1 (4/148-3%) and 8 cases were negative (8/148-5.5%).

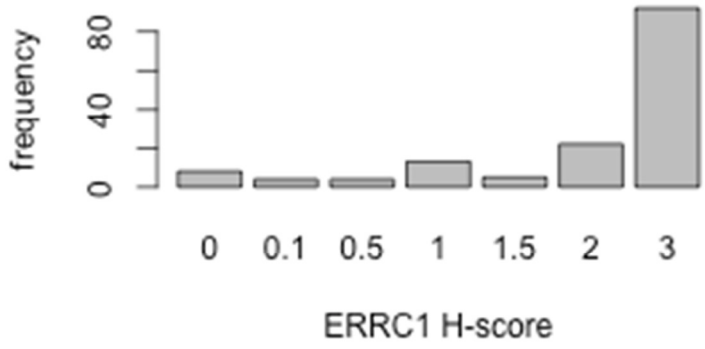

Figure 16ERCC1 H-score values distribution. 92 cases showed a 3 value, 22 cases 2, 5 cases 1.5, 13 cases 1, 4 cases 0.5, 4 cases 0.1 and 8 cases were negative.

According to H-score values we divided the cases in two groups: ERCC1 positive (H-score ≥0.1) and ERCC1 negative (H-score =0); 140 patients were ERCC1 positive, 8 were negative. As shown in Table 4, the two groups were correlated with clinical and pathological features: age, gender, asbestos exposure, histotype, status (dead-alive) and treatment, by Fisher's exact test. We found a significant correlation between the ERCC1 protein expression and the status (P=0.008): ERCC1 negative patients had a better prognosis than the ERCC1 positive. We performed the same statistical analysis using the median H-score value (3) as cutoff, but no significant correlations were found. Analysis of survival showed a significant correlation between ERCC1 protein expression and DSS positive (H-score ≥0.1 ; 141/148, 95%) and 7 ERCC1 negative (H-score=0; 7/148, 5%) (Figure 17): patients with negative ERCC1 had a significantly better outcome when compared with the group with positive ERCC1 (Logrank test P=0.004) (Table 4). The same result was obtained in the subgroup of patients treated with platinum alone or in combination with alimta (n=110) (Logrank P=0.01), when we divided the population in two groups according to the H-score: ERCC1 negative (H-score=0; 8/110) and ERCC1 positive (H-score ≥0.1; 102/110) (Figure 18.).

	ERCC1 H-score		P-value (Fisher exact test)	ERCC1 mRNA		P-value (Kruskal-Wallis test)
	Positive (H-score≥0.1)	Negative (H-score=0)		≥ median value	< median value	
TOT PATIENTS	140 (94.5%)	8 (5.5%)		57 (49.6%)	58 (50.4%)	
Age classes						
(27, 62]	29	3	0.66	13	10	0.72
(62, 70]	35	2		14	13	
(70, 75]	36	1		11	18	
(75, 90]	40	2		20	16	
Gender						
Male	95	8	1	42	39	0.36
Female	45	0		16	18	
Asbestos Exposure						
Yes	64	7	0.70	37	34	0.96
No	70	1		21	19	
Unkown	6	0		0	4	
Histological Subtype						
Epithelial	101	7	0.83	38	44	0.87
Biphasic	20	0		8	8	
Sarcomatoid	19	1		12	5	
Status*						
Alive	37	6	**0.008**	14	15	0.85
Dead	100	2		42	42	
Lost at follow up	3	0		2	0	
DSS (dead patients) [2]	9	14	**0.004** [1]	7	10	0.76 [1]
DSS (alive patients) [2]	13 (n=41)	25 (n=6)		17 (n=10)	23 (n=11)	
DSS (dead patients) [2;3]	10.5	14	**0.01** [1]	10.5	9.5	0.54 [1]
DSS (alive patients) [2;3]	12.5 (n=40)	25 (n=6)		16 (n=17)	22.5 (n=12)	
Treatment						
Platinum	26	1	0.29	8	14	**0.04**
Alimta	2	0		1	1	
Platinum+Alimta	73	7		25	33	
None	31	0		18	8	
Unknow	8	0		6	1	

Table 4 ***Correlation between ERCC1 protein and mRNA levels and the clinical pathologic features of MPM patients***.*[1]Logrank test; [2] median value of DSS expressed in months; [3]median value of DSS expressed in months evaluated in the subgroup of treated patients (platinum and platinum plus alimta). The median RQ value was 1.79.*

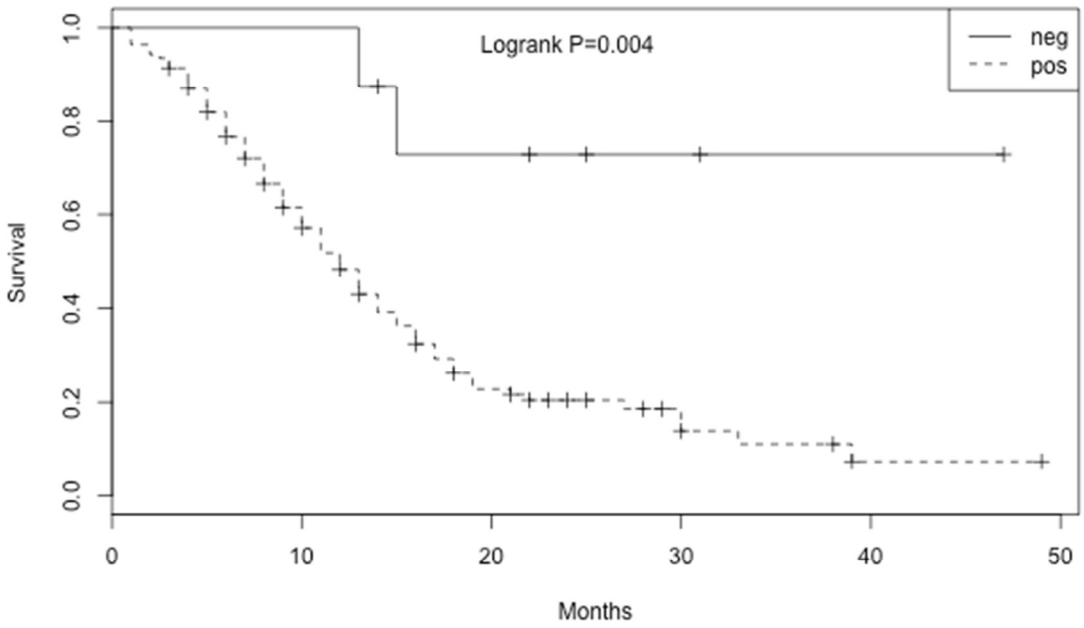

Figure 17 Kaplan-Meier DSS curves in MPM patients showing negative (solid line) and positive (dashed line) ERCC1 protein levels.

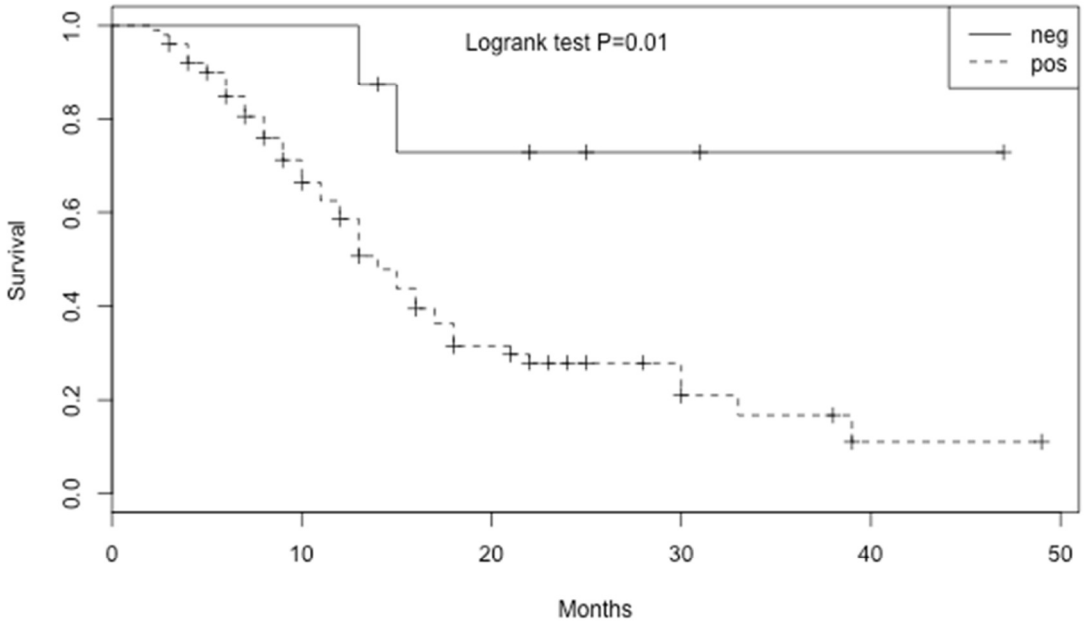

Figure 18 Kaplan-Meier DSS curves in MPM patients treated with platinum or platinum+alimta showing negative (solid line) and positive (dashed line) ERCC1 protein levels.

4.2.4 ERCC1 Gene Expression

ERCC1 mRNA was obtained in 115 cases. We observed very variable values: the median mRNA level value was 3,68 (average value 12.35; range from 0.18 to 163.76). The mRNA expression data were analysed continuously using the median value 3.68 as a cutoff in order to divided the whole population in two groups, ERCC1 positive (RQ ≥3.68, 58/115, 50.4%) and ERCC1 negative (RQ <3.68, 57/115, 49.6%). We correlated, through Kruskal-Wallis test, the two groups with the clinical and pathological features of the patients: age, gender, asbestos exposure, histotype, status (dead-alive) and treatment. As shown in Figure 19, the patients who didn't received treatment (because of advance cancer, poor performance status or age), showed high level or ERCC1 mRNA (P=0.04) (Table 4) compared to those selected for treatment. The comparison between ERCC1 mRNA levels and DSS was not statistically significant in whole population, as well as in the subgroup of treated patients (categorised according to median value of RQ =3.68 and RQ =1.79 respectively) (Table 4).

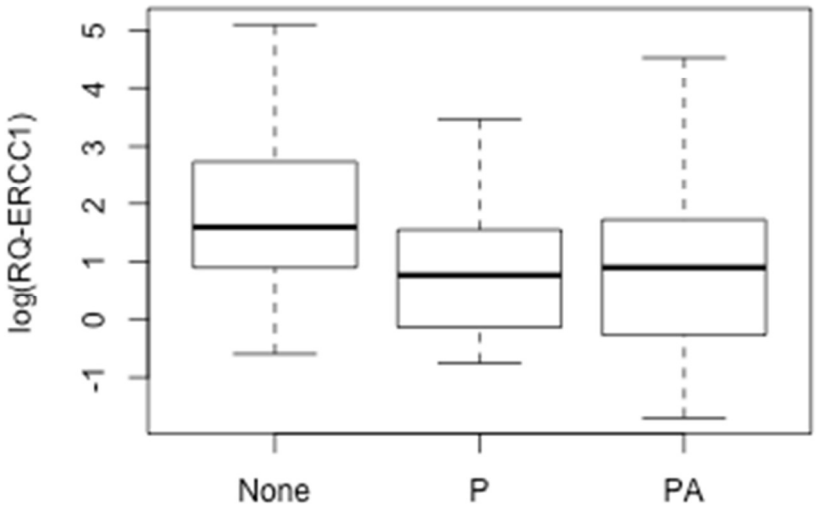

Figure 19 Box plot showing the correlation between ERCC1 mRNA levels and the treatment. P=paltinum; PA=platinum+alimta. We omitted for the analysis the only two cases treated with alimta alone. mRNA levels are expressed as log(RQ).

Finally, as shown in Figure 20, a significant association was found between ERCC1 gene and protein expression, though it is pretty weak (Kendall test, tau =0.21, P=0.032).

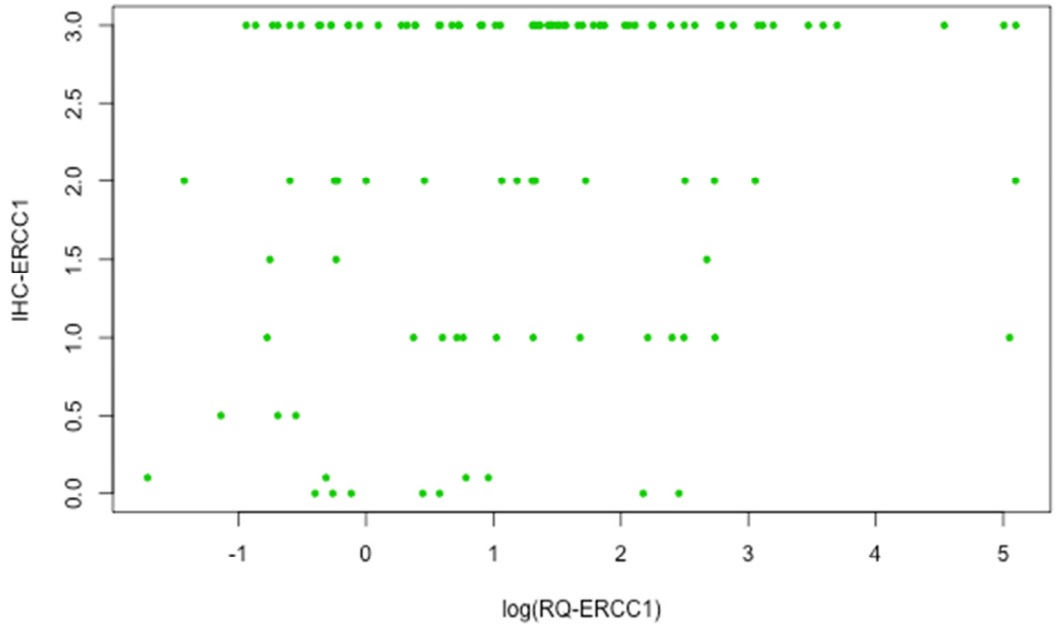

Figure 20 Scatter plot showing the correlation between ERCC1 protein and gene expression. mRNA levels are expressed as log(RQ).

4.2.5 Thymidylate Synthase protein expression.

TS immuno-staining was successfully performed in all the 148 cases. Figure 21 shows the distribution of H-score values: 4 cases showed H-score 3 (3%); 11 cases 2 (7.5%); 15 cases 1.5 (10%); 18 cases 1(12%); 17 cases 0.5 (11.5%); 6 cases 0.3 (4%); 11 cases 0.2 (7.5%); 18cases 0.1 (12%) and 48 cases were negative (32.5%). An example of high and low TS protein expression in MPM is shown in Figure 22. According to the distribution of H-score values we divided the cases in two groups: TS positive (H-score ≥0.1) and TS negative (H-score =0). Out of 148 patients 100 were TS positive (67.5%), and 48 were negative (32.5%). We correlated through Fisher's exact test the two groups with the clinical and pathological features of the patients: age, histotype, gender, asbestos exposure, treatment and status (dead-alive); we did not find any correlation between TS protein expression and the characteristics above reported. Instead, when the whole population was categorised according to median H-score (0.2) (H-score <0.2, 66/145-45.5%; H-score ≥ 0.2, 79/145-54.5%; 3 lost to follow up) we observed a significant correlation between TS protein expression and the status (Fisher's exact test P=0.04), in detail the patients who showed high levels of TS had a better prognosis than the patients with low levels. In order to investigate the prognostic value of TS in MPM patients we performed a survival analysis but we did not find a significant correlation between DSS and TS protein levels. As alimta inhibits TS enzymatic activity we investigated the

predictive value of TS doing a survival analysis on MPM patients treated with alimta alone or in combination with platinum, but no correlation was found between TS protein expression and outcome (Table 5).

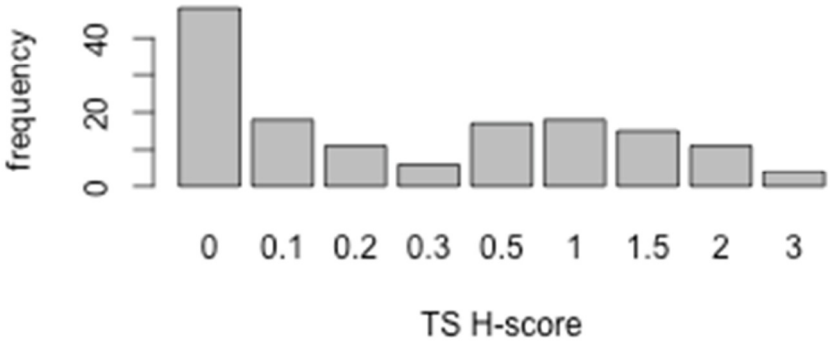

Figure 21 TS H-score values distribution. 4 cases showed a 3 value; 11 cases 2; 15 cases 1.5; 18 cases 1; 17 cases 0.5;6cases 0.3; 11 cases 0.2; 18cases 0.1 and 48 cases were negative.

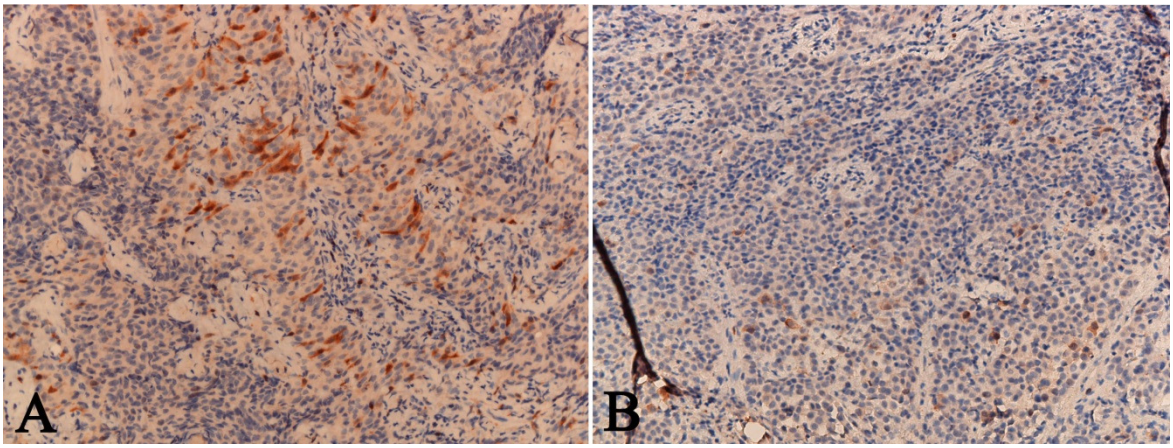

Figure 22 Examples of TS expression in an MPM tumor section stained with anti-TS antibody (clone TS106, dilution 1:50) A) High TS expression B) Low TS expression.

	TS H-score		P-value (Fisher exact test)	TS mRNA		P-value (Kruskal-Wallis test)
	Positive (H score≥0.1)	Negative (H-score=0)		≥ median value	< median value	
TOT PATIENTS	100 (67.5%)	48 (32.5%)		47 (50.5%)	46 (49.5%)	
Age classes						
(27, 62]	22	10	0.51	14	9	0.65
(62, 70]	28	9		10	11	
(70, 75]	25	12		9	14	
(75, 90]	25	17		14	12	
Gender						
Male	70	33	1	33	32	0.41
Female	30	15		14	14	
Asbestos Exposure						
Yes	53	24	0.72	25	26	0.89
No	42	23		22	17	
Unkown	5	1		0	3	
Histological Subtype						
Epithelial	75	33	0.66	30	37	0.30
Biphasic	12	8		7	5	
Sarcomatoid	13	7		10	4	
Status						
Alive	32	11	0.24	9	13	0.49
Dead	65	37		36	33	
Lost to the follow up	3	0		2	0	
DSS (dead patients) [2]	9	10	0.39 [1]	7	10	0.11 [1]
DSS (alive patients) [2]	13 (n=32)	25 (n=11)		18 (n=9)	23 (n=13)	
DSS (dead patients) [2;3]	9	10	0.92 [1]	9	9	0.75 [1]
DSS (alive patients) [2;3]	13 (n=27)	24 (n=9)		18 (n=11)	25 (n=8)	
Treatment						
Platinum	17	10	0.65	8	10	**0.06**
Alimta	2	0		1	1	
Platinum+Alimta	56	24		19	28	
None	19	12		16	5	
Unknown	6	2				

Table 5 Correlation between TS protein and mRNA levels and the clinical pathologic features of MPM patients. *[1]Logrank test, [2]median value of DSS expressed in months; [3]median value of DSS expressed in months evaluated in the subgroup of treated patients (alimta and platinum plus alimta). The median RQ value was 2.77*

4.2.6 TS Gene Expression

TS mRNA levels were successfully evaluated in 93 cases. We obtained very variable values: the median mRNA level value was 4,02, (average value 24,55; range to 0,17 to 615,85). The mRNA expression data were analysed continuously using median value 4,02 as a cutoff to divided the whole population in two groups, TS positive (RQ ≥4.02, 47/93-50.5%) and TS negative (RQ <4.02, 46/93-49.5%). We correlated the two groups with the clinical and pathological features of the patients: age, gender, asbestos exposure, histotype, treatment, and status (dead-alive), using

Kruskal-Wallis test (Table 5). We observed a favourable trend between the TS mRNA levels and the treatment (P=0.06): as shown in Figure 24 the patients who were not selected for treatment had higher level of mRNA than those who were selected for a therapeutic approach. To investigate the prognostic value of TS in MPM patients we performed a survival analysis but we did not find a significant correlation between DSS and TS mRNA levels; notable is the positive trend between DSS and TS mRNA levels until the 30th months (Figure 24). We did not observed a significant correlation between TS gene expression and DSS in the subgroup of treated patients (patients treated with alimta alone or in combination with platinum and categorised according to median value of RQ =2.77) (Table 5).

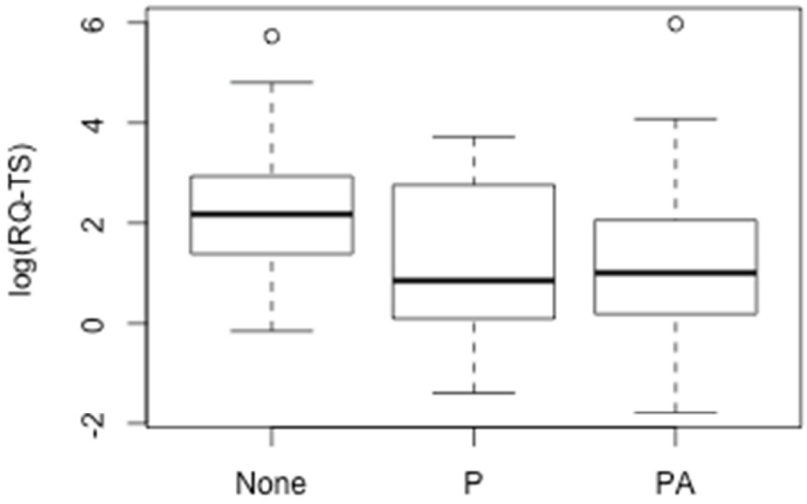

Figure 23 Box plot showing the correlation between TS mRNA levels (expressed as logRQ) and the treatment. P=paltino; PA=platino+alimta. We omitted for the analysis the only two cases treated with alimta alone

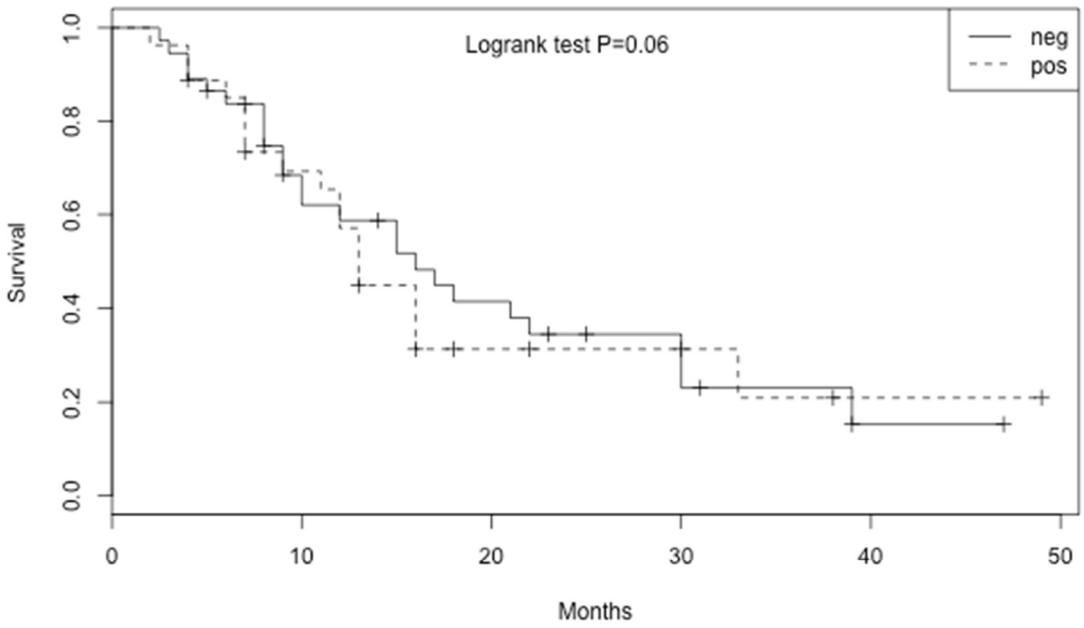

Figure 24 Kaplan-Meier DSS curves in MPM patients with high and low TS mRNA levels. Negative patients (solid line) show low mRNA levels (lower than the median RQ value chosen as cutoff); positive patients (dashed line) show high mRNA levels (higher than the median RQ velue chosen as cutoff).

Furthermore, we studied the correlation between TS gene and protein expression. We performed a correlation analysis and, similarly to ERCC1, a significant association, though not too strong, between the protein and gene expression of TS was identified (Kendall test, tau =0.21, P=0.006) (Figure 25).

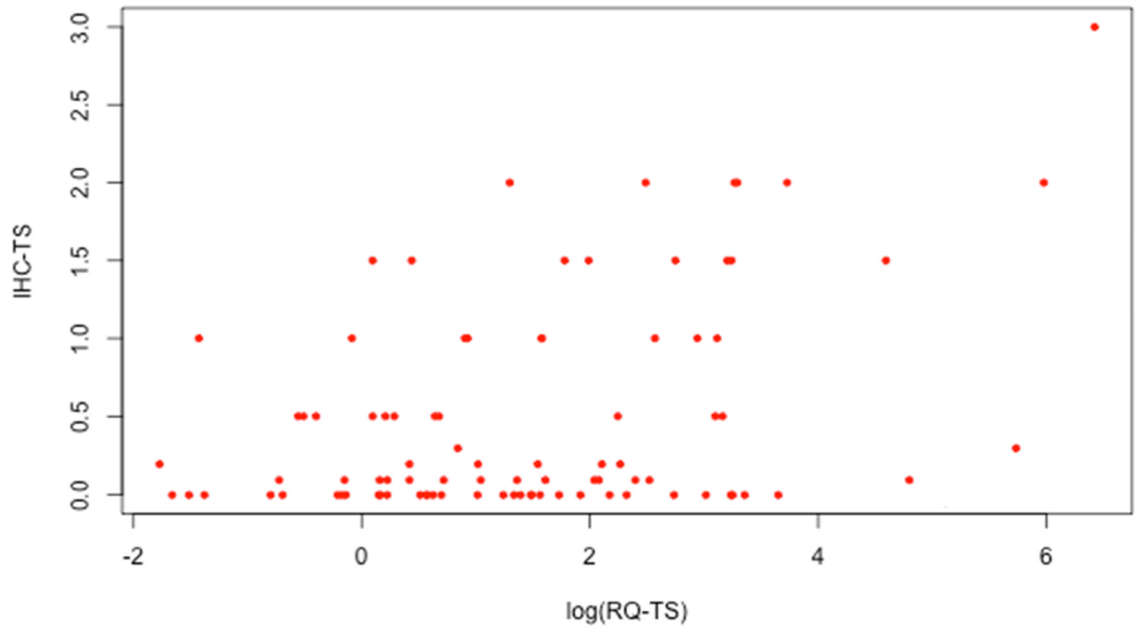

Figure 25 Scatter plot showing the correlation between TS protein and gene expression. mRNA levels are expressed as log(RQ).

By comparing ERCC1 and TS gene and protein expression, we found a statistically significant association in both cases, using respectively Pearson's test (r^2 = 0.88, P=2.2e-16) and Kendall's test (tau =0.16 P=0.01) (Figure 26, Figure 27). The correlation between the TS and ERCC1gene expression results definitely more strong than the protein correlation.

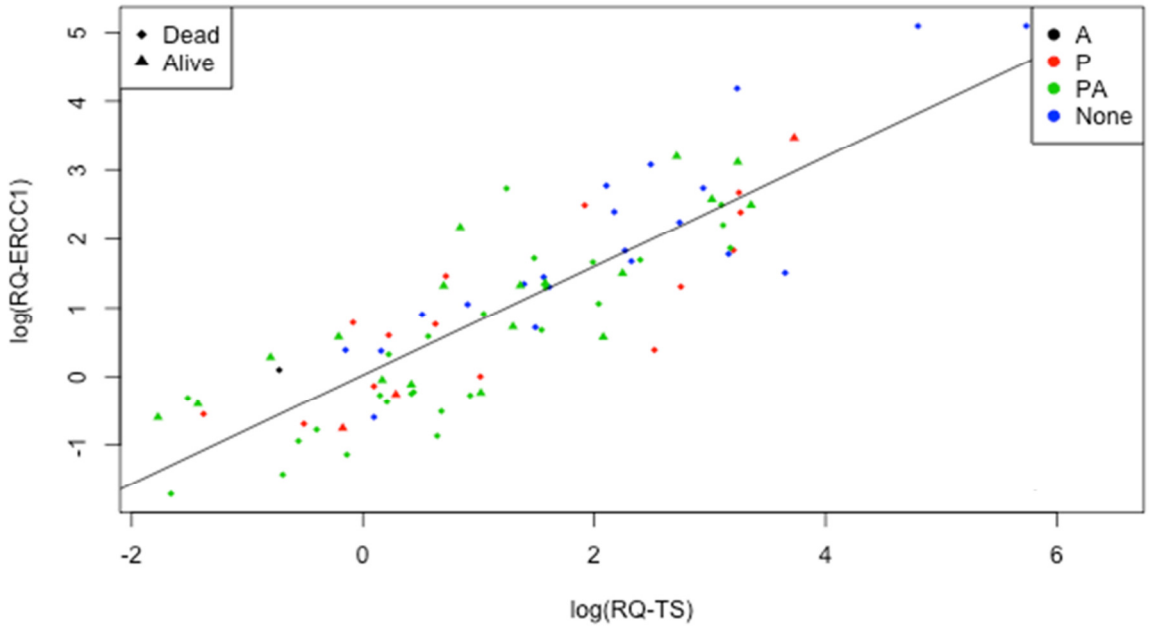

Figure 26 Correlation analysis between ERCC1 and TS mRNA levels
A=alimta; P=platino; PA=platinum+alimta; None=no treatment. mRNA levels are expressed as log(RQ)

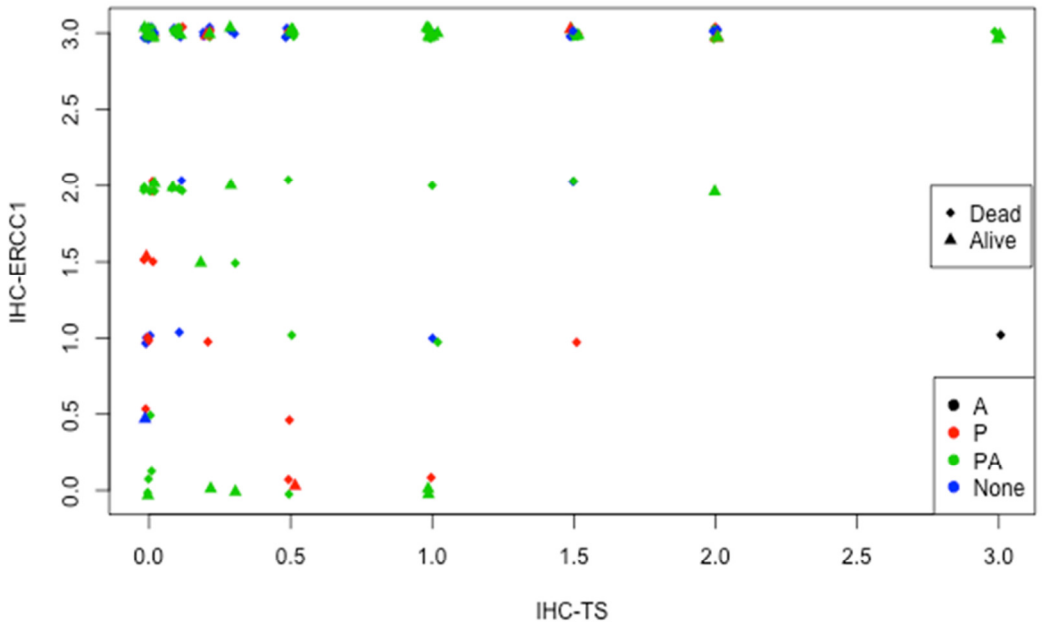

Figure 27 Correlation analysis between ERCC1 and TS protein levels.
A=alimta; P=platino; PA=platinum+alimta; None=no treatment.

4.3 Clonality Assessment

4.3.1 Sensitivity assay

First we established the sensitivity of the HUMARA assay for the detection of under-represented alleles by both gel and capillary electrophoresis: different amounts of mono-allelic (HpaII-digested) and bi-allelic (HpaII non-digested) DNA from the 1290 melanoma monoclonal cell line were mixed in different proportions. PCR products were resolved by electrophoresis in 3% agarose and visualized under UV light in the presence of ethidium bromide, or by capillary electrophoresis and analysed by Genotypic Bioanalyzer (Applied Biosystems) (Figure 28). Linear regression of input vs detected allele ratios revealed a robust correlation (R^2 >0.98), with the less frequent allele detectable when present at a fraction greater than or equal to 1 in 8 (12.5% of the input copies), Figure 29.

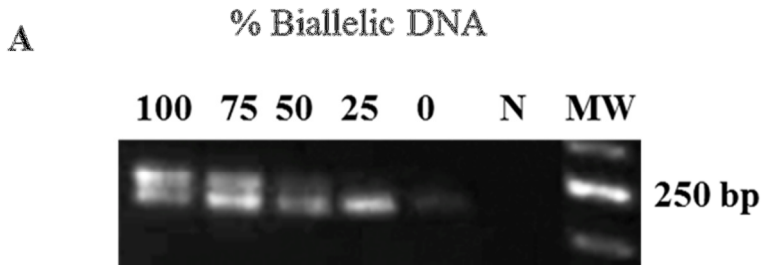

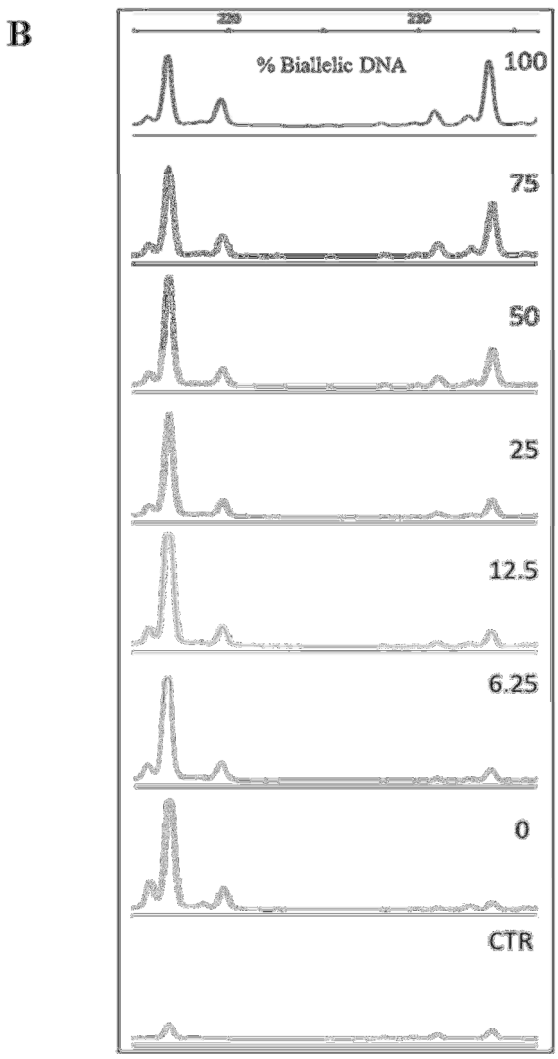

Figure 28 Sensitivity of the HUMARA assay by gel and capillary electrophoresis . *A) Different amounts of HpaII-digested and non-digested DNA from the monoclonal melanoma cell line 1290 were mixed and subjected to PCR for detection of HUMARA locus. PCR products were resolved on a 3% agarose gel containing Ethidium Bromide (0.5 ug/ml) and detected under UV light. The minor allele was visible in PCR reactions containing as little as 25% of the bi-allelic sample. N denotes the no template control. 100, 75, 50, 25 and 0 indicate the percentage of bi-allelic DNA in the PCR reaction.B) PCR products were resolved onto the Applied Biosystems 3100 Genetic Analyser. CTR denotes the no template control. 100, 75, 50, 25, 12.5, 6.25 and 0 indicate the percentage of bi-allelic DNA in the PCR reaction.*

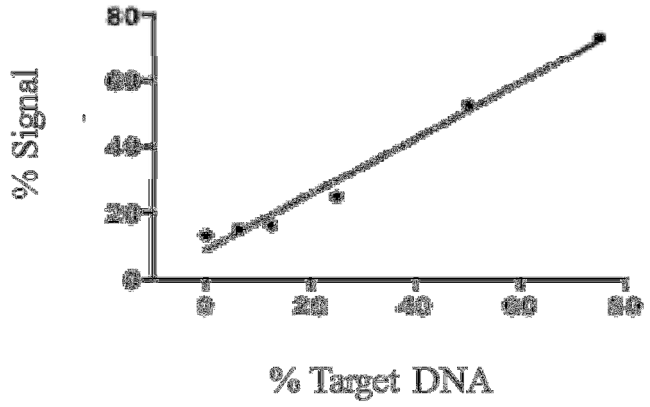

Figure 29 Linear regression analysis calculated with Prism 6 software, shows comparison between input and detected allelic/biallelic ratios calculated using Genescan software. (R^2 >0.98). The minor allele was reliably detectable in PCR reactions containing as little as 25% of the bi-allelic sample.

4.3.2 Clonality analysis.

HUMARA clonality assays were carried out in 14 sporadic and 2 familial (i.e.harbouring BAP1 mutation14), Stage I to III biopsies resected from 14 female MM patients, who underwent surgery (Table 6). In two out of 14 sporadic cases, two distinct nodules were collected and analyzed. Pathological evaluation revealed absence of tumour cells in all the normal microdissected tissues and less that 5% normal infiltrating cells in all microdissected tumour samples included in this study. As a control, we performed HUMARA assay on healthy male DNA (bearing a single unmethylated, active X chromosome), shown as a single PCR band/peak, indicating complete DNA digestion by HpaII enzyme, hence a lack of bias in the HUMARA assay, due to possible incomplete digestion (

Figure *30*). As additional controls, HUMARA assay was also performed on a healthy female DNA sample (L IV-II) and on DNA from a melanoma cell line (#1290, female): as shown in

Figure *30*, gel and capillary electrophoresis successfully detected a polyclonal and a monoclonal pattern, respectively. Samples were classified as non-informative when a single band or peak was detected in the nearby normal tissue, after digestion with the HpaII enzyme, indicating the presence

of skewed lionization, an event that occurs in about 10% of a healthy female population (Vickers *et al*, 2001). Out of 16 samples tested, 14 were informative. We found two non-informative samples: one case (#1359, a sporadic MM) is shown in

Figure 31: PCR amplification of mock-digested DNA produced two bands/peaks, while only one band/peak was observed after treatment with HpaII, indicating skewed (non-random) X chromosome inactivation. In the second case (L-III-18, a familial MM case), PCR amplification of both mock- and HpaII-digested DNA produced a single band, indicating that the lengths of the paternal and maternal alleles were identical (data not shown). Of the 14 informative samples, 13/14 PCR products (93%) displayed two distinct bands and peaks. 11 representative samples are shown in

Figure 31. Corrected Allele Ratio (CR) calculated on the allele peak areas by Genotypic Bioanalyzer was ≥0.3 in all 13 samples indicating a polyclonal origin of MM tumors (

Figure *31* B). Case #524 showed a quite distinct pattern, as one nodule (#524B) revealed a monoclonal pattern (CR ≤0.3), while the other (#524A) was polyclonal.

Sample ID	Age	Inheritance	Histology	Staging	Clonality
6	ND	Sporadic	Biphasic	NA	Polyclonal
61	82	Sporadic	Epithelioid	III	Polyclonal
93	64	Sporadic	Epithelioid	III	Polyclonal
207A	74	Sporadic	Epithelioid	III	Polyclonal
207B					Polyclonal
273	66	Sporadic	Biphasic	III	Polyclonal
524A	72	Sporadic	Epithelioid	III	Polyclonal
524B					Monoclonal
851	58	Sporadic	Biphasic	III	Polyclonal
1250	65	Sporadic	Epithelioid	III	Polyclonal
1359	56	Sporadic	Epithelioid	III	Non-informative
1419	25	Sporadic	Biphasic	III	Polyclonal
LIII18	64	Familial	Epithelioid	III	Non-informative
R088	59	Sporadic	Epithelioid	III	Polyclonal
R693	63	Sporadic	Epithelioid	I	Polyclonal
WIII6	66	Familial	Epithelioid	II	Polyclonal

Table 6 Clinical features and clonality pattern in 16 biopsies from 14 MM female patients.

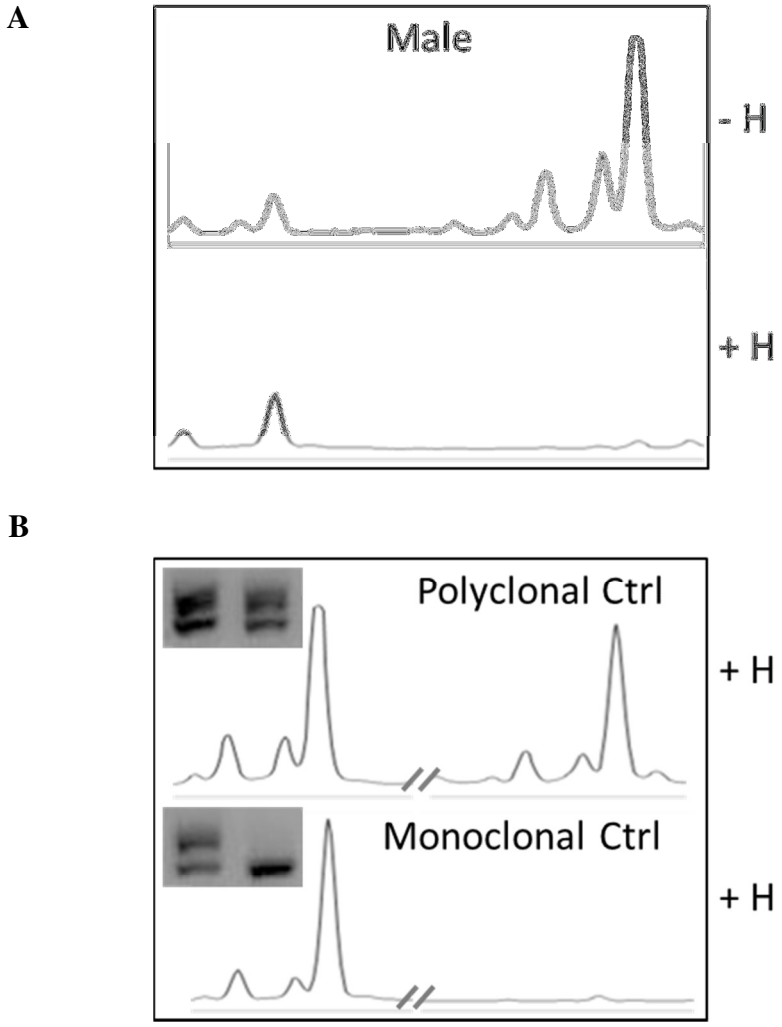

Figure 30 Quality controls. A*) Humara-PCR was performed on HpaII-digested (H+) and mock-digested (H-) DNA from a healthy male and analyzed by capillary electrophoresis, using the 3100 Genome analyzer. Presence of a single PCR peak indicated complete DNA digestion by HpaII enzyme. B) Healthy female DNA sample (L-IV-II) and DNA from a human monoclonal melanoma cell line (#1290, female) were subjected to HUMARA assay. Capillary electrophoresis successfully detected a polyclonal pattern and a monoclonal pattern*

A

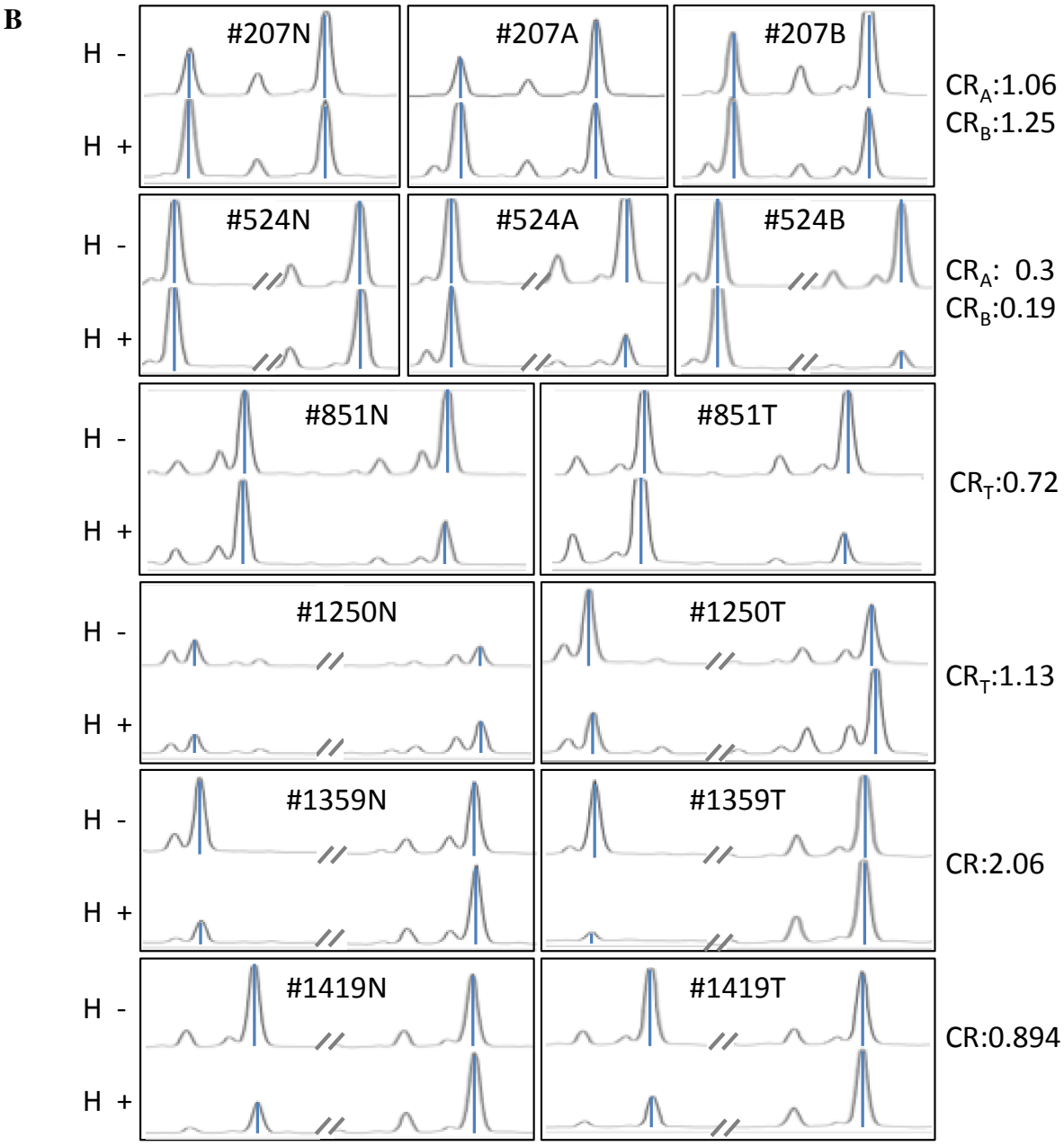

Figure 31X chromosome inactivation analysis by HUMARA assay shows both monoclonal and polyclonal pattern of Malignant Mesotheliomas. Gel electrophoresis *A) and Capillary Electrophoresis B) Analysis of a panel of representative MM samples. 100 ng of DNA from tumor and adjacent normal tissue were digested with 10 U Hpa II restriction enzyme overnight at 37◦C. Separate aliquots of DNA were subjected to mock digestion without the enzyme. Digested and mock-digested DNA were submitted to PCR reaction for detection of the HUAMRA locus as described above. Gel electrophoresis A). PCR products from mock digested (H-) and HpaII-digested (H+) samples were separated on a 3% agarose gel and visualized under UV light, using ethidium bromide. B) Capillary Electrophoresis. HUMARA PCR assay was performed using a 5FAM-labeled forward primer, and quantified by the Applied Biosystems 3100 Genetic Analyser. Two major peaks marked with the blue bar denote the two allelic HUMARA loci amplified in PCR HpaII-digested (H+) and mock-digested samples (H-). The allele intensities were measured as peak area of both alleles, which is proportional to the molar amount of DNA. Peak areas were calculated for each allele by using Genescan software, as described in the Material and Methods section. N denotes normal nearby tissue samples, while T indicates the tumor samples. A and B indicate independent tumor nodules obtained from the same patient. Sample #1359 was analyzed as a non-informative sample, as a single band/peak (CR=2.06) was detected after HpaII digestion of the normal tissue counterpart indicating a skewing of the X-chromosome inactivation.*

5 DISCUSSION

5.1 Mutational analysis of EGFR and downstream pathway in pleural malignant mesothelioma samples.

As EGFR is involved in the carcinogenesis of MPM, it is possible that EGFR-targeted therapies may be efficacious in MPM patients (Barbieri *et al*, 2011). EGFR TKI inhibitors, such as gefitinib and erlotinib, inhibit MPM cell migration and proliferation, enhance the response to radiation of human MPM cell lines, and reduce motility and invasion in MPM cell lines (Kurai *et al*, 2012). However, the promising results obtained in *in vitro* studies were not reproduced in two phase II trials involving patients with pleural and peritoneal mesotheliomas, although it should be noted that neither study evaluated the mutation status of the *EGFR* gene and its downstream signalling transduction pathway (Garland *et al*, 2007; Govindan *et al*, 2005). As in the case of colorectal cancer and lung adenocarcinoma, this lack of molecular selection could explain the therapeutic failure. The few studies that have sought mutations in the tyrosine kinase domain of the *EGFR* gene in patients with malignant mesotheliomas involved small populations and used a relatively insensitive method (the direct sequencing of exons 18-21) (Cortese *et al*, 2006; Enomoto *et al*, 2012; Velcheti *et al*, 2009). The primary objective of the first part of our study was to look for *EGFR* gene mutations in a larger series of patients (n=77) using two molecular methods: all of the cases were first screened using Scorpion-ARMS technology, which is capable of detect 1% of mutated cells against a 99% background of wild-type cells, followed by direct sequencing in order to find rarer mutations or mutations that cannot be detected using the first method. However, despite this, we did not find any mutations in the TK domain of *EGFR*: in addition to confirming previous findings (Cortese *et al*, 2006; Velcheti *et al*, 2009), this also indicates that, unlike in the case of lung adenocarcinomas, mutations cannot be detected even when real-time PCR is used to increase sensitivity (Allegrini *et al*, 2012). On the contrary, Enomoto *et al*. have recently studied 38 patients and found *EGFR* missense mutations in exons 18 (n=1), 20 (n=3) and 21 (n=1) in six (16%) patients with pleural (n=3) or peritoneal mesotheliomas (n=3) (Enomoto *et al*, 2012). *EGFR* gene mutations have been previously found in peritoneal mesotheliomas (Foster *et al*, 2009; Foster *et al*, 2010), but this is the only published report of *EGFR* gene mutations in MPM. However, the study involved Japanese patients, who are characterised by more frequent *EGFR* gene mutations in lung adenocarcinoma than Western patients (Endo *et al*, 2005). Furthermore, some of the detected mutations had never been reported before, and their biological and clinical significance is still unknown. An alternative method of blocking EGFR is to use monoclonal antibodies (mABs), which

may be extremely useful as it has been demonstrated that MPM patients show *EGFR* gene amplification (Dazzi *et al*, 1990; Destro *et al*, 2006; Okuda *et al*, 2008). No published studies have assessed the *in vivo* effects of anti-EGFR mAbs on MPMs, although one recent study has found that cetuximab is highly efficacious in cultured MPM cell lines (Kurai *et al*, 2012). It has been demonstrated that mutations in EGFR downstream pathways can affect the efficacy of EGFR mABs in other tumours such as colorectal adenocarcinoma) (Jonker *et al*, 2007), and we found nine patients (11.7%) with missense mutations involving the *KRAS* (n=5), *BRAF* (n=3) and *PIK3CA* genes (n=1). Few other studies have separately investigated the presence of mutations in *KRAS*, *BRAF* and *PIK3CA* genes in MPM samples and mesothelioma cell lines without success (see review by Argawal *et al*., 2010) but, to the best of our knowledge, ours is the first to investigate these alterations systematically in a large series of MPM patients. Various reasons may explain these discrepant results. We screened a large number of samples (n=77), whereas the other studies were based on smaller series and may have underestimated the real frequency of such mutations. Furthermore, we analysed *KRAS* gene mutations using a mutant-enriched PCR (ME-PCR) technology whose sensitivity is 0.1% (Molinari *et al*, 2011), and so it is possible that the percentage of *KRAS* gene mutated cells is very low in MPM and that more widely used sequencing methods are unable to detect small clones. Our findings show that, although infrequent, mutations in EGFR downstream pathways can be found in MPMs, thus supporting the hypothesis that EGFR mABs may be clinically effective in the majority of patients. On the other hand, patients with a molecular profile indicating putative resistance to EGFR mABs (because of the presence of *KRAS* or *BRAF* or *PIK3CA* mutations) may be directed towards new targeted therapies. One recent study has shown vemurafenib is promising not only in patients with metastatic melanoma, but also in patients with non-small lung cell cancer carrying a *BRAF* mutation (Gautschi *et al*, 2012), and selumetinib and BYL-719, which target *KRAS* and *PIK3CA* mutations are currently being evaluated in several clinical trials (Clinical Trials Magnifier). Our data therefore underline importance of the molecular characterisation of patients with MPM. The clinical implications of the gene mutations detected in our study are not clear. DSS was no different in the patients with or without gene mutations (whether analysed together or separately). Interestingly, all of the patients with *KRAS* gene mutations reported occupational asbestos exposure, but none of those with *BRAF* or *PIK3CA* gene mutations. Comparison of mean DSS in the *KRAS* and *BRAF* gene mutated patients *vs* wild-type patients previously exposed to asbestos or not showed that the *KRAS* gene mutated patients (n=5) tended to have a worse prognosis than the wild-type patients (9.20 ± 6.91 *vs* 15.6 ± 10.39 months), and the *BRAF* gene mutated patients (n=3) tended to have a better prognosis (20.33 ± 12.06 *vs* 12.1 ± 8.37 months). However, the differences were not statistically significant and our findings need to

be confirmed in larger series of MPM patients. In conclusion, our extensive molecular characterisation of EGFR pathways may explain the failure of TKI administration and may open up the possibility of developing new targeted therapies.

5.2 Prognostic and predictive biomarkers in malignant pleural mesothelioma.

Malignant pleural mesothelioma is a disease with high resistance against different forms of oncology therapy. The combination of platinum (cisplatin/carboplatin) and pemetrexed represents the standard of care in the first-line treatment of MPM. However, more than one third of patients do not respond to this schedule and are exposed to useless toxicity. It is now recognized that the way a patient responds to chemotherapy is a complex trait, influenced by the tumour characteristics and individual genetic constitution: therefore, patient selection on the basis of prognostic and predictive biomarkers is crucial for maximising therapeutic efficacy and minimising useless treatment. The aim of this study was to find valid biomarkers to select patients who can receive more advantage from the treatment with standard chemo agents. On the basis of previous studies carried out on NSCLC, we selected ERCC1 and TS for our investigation and we evaluated prognostic and predictive value of both protein and transcript level. Since platinum acts through the formations of adducts to DNA and ERCC1 is involved in mechanisms of DNA repair (NER system), the initial hypothesis was that low levels of ERCC1 in tumour cells should be related to A) high response rate in patients treated by platinum based chemotherapies, and B) decrease survival in untreated patients due to the reduced ability to repair the DNA damages. Conversely, high levels of ERCC1 might be related to resistance to platinum therapy and improved outcome in non-treated patients. We evaluated ERCC1 levels in tumour cells through the analysis of protein expression, by means of immunohistochemistry -a technic used in most pathology laboratories- or by gene expression assessment obtained by mRNA extraction and amplification. The latter method gives a more accurate information even if it is quite difficult to perform in routinely treated samples. We performed both analyses in an effort to identify the more reliable method and to compare the results of both analyses with the main prognostic and predictive parameters. Firstly we noticed that in those patients not selected for any treatment because of poor performance status, advanced cancer or age, both ERCC1 and TS showed high mRNA levels. A possible explanation could be that in advanced MPM tumor cells have a high division rate, TS is strongly activated, as it is involved in DNA synthesis. At the same time, in the high proliferative cells, DNA damages occurs more often than in the normal cells thus causing a strong activity of the enzymes involved in the DNA repair, such as ERCC1. Statistical analysis carried out on ERCC1 showed that patients negative for its protein

expression had significant better survival (evaluated by alive-dead and by DSS) than those who were ERCC1 positive, independently from the intensity of staining (evaluated as H-score). These results were obtained both in the whole cohort (n=148) and in the subgroup of the treated patients (n=110). Since the latter group was more numerous than the group of non-treated patients, the result seems to indicate that the lack of expression of ERCC1 appears to have a predictive rather than a prognostic significance and it should be used to identify patients eligible for platinum based treatment. On the contrary, the statistical analysis of ERCC1 gene expression did not show any prognostic and predictive significance. The discrepancy in the correlation to survival between protein and gene expression could be explained by the fact that we found a weak correlation between ERCC1 gene and protein expression, this suggests a possible control mechanism at the translational level of the synthesis of this enzyme, or a control of protein turnover. Numerous studies, performed in several solid organ tumours, demonstrated that ERCC1 mRNA levels predict response to treatment and/or survival . For example, high levels of ERCC1 mRNA in pre-treated ovarian and gastric tumour tissue have been associated with platinum resistance (Dabholkar *et al*, 1994; Metzger *et al* 1998). Similarly, in non-small cell lung cancer (NSCLC), in patients treated with platinum-based chemotherapy, low or undetectable levels of ERCC1 mRNA, or protein expression predict better survival (Lord *et al,* 2002; Olaussen *et al*, 2006). Recently Zucali *et al* have investigated the role of ERCC1 protein and gene expression in a series of 63 patients with MPM treated by standard chemotherapy finding no association with the outcome; similar results were also obtained by Righi *et al* in a study performed on 60 MPM patients. Our results, obtained in a larger series of MPM specimens, suggest that ERCC1 protein evaluation by immunohistochemistry could represent a useful tool to select patients potentially responding to chemotherapy. Pemetrexed (alimta) inhibits multiple enzymes in the folate metabolic pathway, and thymidylate syntase (TS) is the main target (Shih et al, 1997). In NSCLC cell lines, high baseline TS gene expression levels conferred resistance to pemetrexed (Giovannetti et al. 2007) and TS levels were correlated to pemetrexed efficacy in a variety of solid tumors (Gomez et al, 2006, Rose et al, 2002). TS mRNA and protein expression levels might also play a prognostic role, as reported in patients with NSCLC (Shintani *et al*, 2003; Hashimoto *et al*, 2006). In our study the correlation between TS protein expression and status (dead-alive) was evaluated by using two parameters (positive *Vs* negative staining and under *Vs* above median H-score value). No correlation was found with survival when patients were divided in positive and negative. In contrast, when the median H-score value of 0.2 was selected, a significant correlation with the status was found, indicating that patients with low levels of TS protein had a higher mortality than those with high TS protein levels, thus assuming a negative prognostic value. TS gene expression did not show any statistically

significant correlation either with patient status and DSS. However, the Kaplan-Meier curves showed a favorable trend for patients with low levels of mRNA (lower than cutoff = 4.02) up to the 30th month of follow up indicating a tendency to predict a positive response to the treatment with alimta alone or in combination. So far, only Zucali *et al* established a significant predictive correlation between low TS mRNA levels and longer overall survival in treated patients. To conclude, the role of TS assessment is worth of prospective validation in future studies on MPM, moreover we plan to further investigate the gene expression of TS and ERCC1 in a wider number of MPM cases to obtain more accurate data and to set up prospective studies in order to confirm the potential role of ERCC1 as a predictive and prognostic biomarker in MPM patients.

5.3 Evaluation of clonal origin of malignant mesothelioma.

Malignant mesothelioma (MM) is a lethal cancer affecting approximately 3,200 individuals each year in the US, most of whom die within 1 year from diagnosis. At diagnosis MMs are histologically complex, comprising different histologic types, epithelioid, sarcomatoid and biphasic, and among them there are also subtypes with distinct histologic characteristics. Diagnosis is further complicated by the presence of intra-tumoural pleomorphism and phenotypic heterogeneity, raising the question of whether MM result from genetic and epigenetic alterations which drive clonal tumour evolution into these different morphologies, or whether mesotheliomas arise from different subsets of mesothelial cells that become malignant more or less at about the same time. Multistep carcinogenesis is the currently accepted hypothesis to explain genetic diversity in tumours (Aparicio *et al*, 2013; Greaves *et al*, 2012).This hypothesis is based on the idea that somatic mutations are rare events: during the process of cellular transformation and development of a neoplasm, multiple genetic events are known to accumulate in the neoplastic cells. However, it is unlikely that multiple events occur in a single cell. Although clonal evolution of cancer is likely to occur irrespective of its origin, identifying whether a tumour is monoclonal or polyclonal at start, have critical implications in terms of early therapeutic intervention. A tumour is considered monoclonal when all cells within the tumour can be traced back to a single progenitor/initiator cell. A tumour which is polyclonal at origin, on the other hand, derives from the concomitant transformation of two or more different ancestor cells. To the best of our knowledge the clonal origin of MM has never been investigated, and MM are assumed to be "clonal" as tumours are generally assumed to be mostly clonal. When patients with very early stage of MM (Stage Ia), such as individuals affected by the BAP1 cancer syndrome, are examined, the presence, even at such an early stage, of many minuscule pleural

nodules (~1 mm in max diameter), has been noted. The finding of multiple pleural nodules in a patient at the earliest possible MM stage raised the question of whether these nodules represented independent growth processes. According to the current dogma, based on the hypothesis of tumour monoclonality, it should be instead that a single monoclonal tumour nodule shed cells in the pleural space that subsequently seeded the pleura. To address whether MM have monoclonal or polyclonal origin, we performed the HUMARA assay (Allen *et al*, 1992). Of the 14 informative samples, 13/14 PCR products (93%) displayed two distinct bands and peaks. Surprisingly, one case (#524) showed a quite distinct pattern, as one nodule (#524B) revealed a monoclonal pattern (CR $\leq$0.3), while the other (#524A) was polyclonal. This finding may indicate that, within a largely polyclonal tumour, composed by clones derived from different cells of origin, a particular clone dominates a certain area. Different hypothesis may be proposed to explain this finding. X-chromosome inactivation based assays may detect a seemingly monoclonal tumour when transformation occurs in multiple cells with the same inactivated X chromosome. Although possible, this is a rare event, mainly dependent on the X-inactivation patch size, due to occurrence of lyonization early in development, which leads few of the progeny of a single embryonic stem cell to be grouped together in the adult, forming patches. A similar phenomenon has been described in breast tissues, which display a rather large patch size (Novelli *et al,* 2003). Alternatively, a true monoclonal nodule may result from the clonal outgrow of a cell which acquired a proliferative advantage. An example is the loss of X-linked FOXP3 gene found in breast and prostate cancer (Zuo *et al*; 2007 Wang *et al*, 2009) Surprisingly, loss of one of the few known X-linked tumour suppressor genes, GPC3, has already been associated to malignant mesothelioma (Murthy *et al,* 2000). In collaboration with the Hawaii Cancer Center, we are currently investigating the status of X-linked tumour suppressor genes in samples #524B compared to #524A and other polyclonal MM tumours. In conclusion, our data indicate that MM may arise as polyclonal tumours due to concurrent transformation of multiple mesothelial cells. X-chromosome studies conducted in some other cancer types indicating a polyclonal origin in some breast and colon carcinomas (Parsons B., 2008; Xin L., 2013), support our findings that not all tumours are monoclonal. The notion that tumours derive from a single cell through the expansion and evolution of several clones has survived almost unchallenged till present. Accordingly, much effort has been placed in dissecting the clonal relationships present within single tumours (Aparicio *et al*, 2013). Our finding that MM are polyclonal at the origin indicates that MM are likely to be clonally complex at the outset. This suggests that not only clonal cancer evolution, but also polyclonal origin of tumours contribute to the intra-tumoural heterogeneity and emergence of drug-resistant subpopulations. A critical implication of this finding is that only tracking the clonal evolution of tumours may not be sufficient to successfully target MM tumours, providing a

possible explanation for the peculiar resistance of MM to current therapies. Instead there is a need to attack simultaneously several different molecular targets, even at early stages of MM development, to eliminate unrelated cell clones, carrying their own distinct set of molecular alterations. Our findings may explain why patients whose tumours are removed at Stage Ia often experience MM recurrence a few years after surgery, in spite of apparent successful tumour eradication. In contrast to the current thinking, recurrence likely represents novel malignancies occurring on other areas of the pleura because of the carcinogenic “field effect” of asbestos and of other mineral fibers and/or because of ubiquitous genetic predisposition. The findings present in this study are relevant to the understanding of human cancer development, and provide a new standpoint for development of effective cancer treatments.

REFERENCES

Ali SH, De Caprio JA, *Cellular transformation by SV40 large T antigen: Interactions with host proteins.* Semin Cancer Biol 2001 11:15-22.

Allegrini S, Antona J, Mezzapelle R, et al *Epidermal growth factor receptor gene analysis with a highly sensitivity molecular assay in routine cytologic specimens of lung adenocarcinoma*. Am J Clin Pathol 138: 377–381.

Allen RC, Zoghbi HY, Moseley AB, et al., *Methylation of HpaII and HhaI sites near the polymorphic CAG repeat in the human androgen-receptor gene correlates with X chromosome inactivation*. Am J Hum Genet 1992 51, 1229-39.

Amin AM, Mason C, Rowe P, *Diffuse malignant mesothelioma of the peritoneum following abdominal radiotherapy*. Eur J Surg Oncol, 2001. 27(2): p. 214-5.

Aparicio S, Caldas C, *The implications of clonal genome evolution for cancer medicine*. N Engl J Med 368, 842-51, 2013.

Ault JG, Cole RW, Jensen CG, et al. *Behavior of crocidolite asbestos during mitosis in living vertebrate lung epithelial cell*s. Cancer Res. 1995;55:792-8.

Barbieri F, Wurth R, Favoni RE, et al (2011) *Receptor tyrosine kinase inhibitors and cytotoxic drugs affect pleural mesotelioma cell proliferation: insight into EGFR and ERK1/2 as antitumor targets*. Biochem Pharmacol 82: 1467–1477.

Benvenuti S, Frattini M, Arena S, et al. *PIK3CA cancer mutations display gender and tissue specificity patterns*. Hum Mutat. 2008;29:284-8

Benvenuti S, Sartore-Bianchi A, Di Nicolantonio F, et al. *Oncogenic activation of the RAS/RAF signaling pathway impairs the response of metastatic colorectal cancers to anti-epidermal growth factor receptor antibody therapies*. Cancer Res 2007;67:2643-8.

Besson A, Robbins SM, Yong VW, *PTEN/MMAC1/TEP1 in signal transduction and tumorigenesis*. Eur J Biochem. 1999;263:605-11.

Beutler E., Yeh M, Fairbanks VF, *Normal human female as a mosaic of X-chromosome activity: studies using the gene for G6PD deficiency as a marker*. Proc. Nati. Acad. Sci. USA, 1962 48: 9-16.

Bocchetta M, Miele L, Pass HI, et al*., Notch-1 induction, a novel activity of SV40 required for growth of SV40-transformed human mesothelial cells. Oncogene*, 2003. 22(1): p. 81-9.

Bogdan S, Klambt C. *Epidermal growth factor receptor signaling*. Curr Biol 2001;11:R292–5.

Bohanes P, Labonte MJ, Lenz HJ. *A review of excision repair cross-complementation group 1 in colorectal cancer,* Clin Colorectal Cancer. 2011 Sep;10(3):157-64. doi: 10.1016/j.clcc.2011.03.024. Epub 2011 Apr 28.

Bollag G, Hirth P, Tsai J, Zhang J et al. *Clinical efficacy of RAF inhibitor needs broad target blockade in BRAF-mutant melanoma*. Nature. 2010 Sep 30;467(7315):596-9. doi: 10.1038/nature 09454.

Boutin C, Dumortier P, Rey F, et al. *Black Spots concentrate oncogenic asbestos fibers in the parietal pleura.* Am J Respir Crit Care Med 1996, 153:444-449.

Boutin C, Schlesser M, Frenay C, et al., *Malignant pleural mesothelioma*. Eur Respir J. 1998;12:972–81.

Boutin C, Viallat JR, Van Zandwijk N, et al. *Activity of intrapleural recombinant gamma-interferon in malignant mesothelioma.* Cancer 67: 2033-2037, 1991.

Britton M. *The epidemiology of mesothelioma.* Semin Oncol 2002, 29: 18-25.

Brown CJ, et al., *The human XIST gene: analysis of a 17 kb inactive X-specific RNA that contains conserved repeats and is highly localized within the nucleus*. Cell, 1992. 71(3): p. 527-42.

Cacciotti P, Libener R, Betta P, et al., *SV40 replication in human mesothelial cells induces HGF/Met receptor activation: a model for viral-related carcinogenesis of human malignant mesothelioma*. Proc Natl Acad Sci U S A, 2001. 98(21): p. 12032-7.

Cappuzzo F, Gregorc V, Rossi E, et al. *Gefitinib in pretreated non-small-cell lung cancer (NSCLC): analysis of efficacy and correlation with HER2 and epidermal growth factor receptor expression in locally advanced or metastatic NSCLC*. J Clin Oncol 2003;21:2658—63.

Carbone M, Emri S, Dogan AU, et al. *A mesothelioma epidemic in Cappadocia: scientific developments and unexpected social outcomes*. Nat. Rev. Cancer 2007, 7, 147–154.
Carbone M, Kratzke RA, and Testa JR, The Pathogenesis of Mesothelioma. Seminars in Oncology 2002, Volume 29, Issue 1 , Pages 2-17.

Carbone M, Ly BH, Dodson RF, et al. *Malignant mesothelioma: Facts, myths and hypotheses.* J. Cell. Physiol., doi:10.1002/jcp.22724 (published online 16 March 2011).

Carbone M, Rizzo P, Grimley PM, et al, *Simian virus-40 large-T antigen binds p53 in human mesotheliomas.* Nat Med, 1997. 3(8): p. 908-12.

Carbone M, Yang H, Pass HI, et al., *BAP1 and cancer* Nat Rev Cancer. 2013 Mar;13(3):153-9.

Carbone M., Izzettin BY, Bertino P, et al, *Erionite exposure in North Dakota and Turkish villages with mesothelioma.* Proc Natl Acad Sci U S A, 2011. 108(33): p. 13618-23.

Carmichael J, Degraff WG, Gamson J, et al. *Radiation sensitivity of human lung cancer cell lines*. Eur J Cancer Clin Oncol 1989, 25: 527-534

Carpenter GKJL, Morrison MM, Cohen S, *Characterization of the binding of I25l-labeled epidermal growth factor to human fibroblasts*, J Biol Chem, 250 (1975), pp. 4297–4304.

Case Records of the Massachusetts General Hospital (case 33111). N Engl J Med 1947, 236:407-412.

Chattopadhyay S, Moran RG, Goldman ID. *Pemetrexed: biochemical and cellular pharmacology, mechanisms, and clinical applications.* Mol Cancer Ther 2007;6:404–17.

Chirieac LR, Corson JM. *Pathologic evaluation of malignant pleural mesothelioma*. Semin Thorac Cardiovasc Surg. 2009;21:121–4.

Ciardiello F, Tortora G. *EGFR antagonists in cancer treatment*. N Engl J Med 2008;358:1160–74.

Cicala C, Pompetti F, Carbone M, *V40 induces mesotheliomas in hamsters*. Am J Pathol 1993, 142(5):1524-1533.

Citri A, Yarden Y. *EGF-ERBB signalling: towards the systems level*. Nat Rev Mol Cell Biol 2006;7:505–16

Cohen S, *Purification of a nerve-growth promoting protein from the mouse salivary gland and its neuro-cytotoxic antiserum*, Proc Natl Acad Sci USA 1960;46:302–11.

Cohen S, Ushiro H, Stoscheck C, et al. *A native 170,000 epidermal growth factor receptor-kinase complex from shed plasma membrane vesicles*. J Biol Chem. 1982;257:1523-31

Cortese JF, Gowda AL, Wali A, et al*, Common EGFR mutations conferring sensitivity to gefitinib in lung adenocarcinoma are not prevalent in human malignant mesothelioma*. Int J Cancer. 2006;118:521-2.

Cunningham D. *Cetuximab (Erbitux) – an emerging targated therapy for epidermal growth factor receptor*. Int J Clin Pract 2004;58:970-6.

Dabholkar M, Vionnet J, Bostick-Bruton F, et al., *Messenger RNA levels of XPAC and ERCC1 in ovarian cancer tissue correlate with response to platinum-based chemotherapy*. J Clin Invest 1994;94:703–708.

Davies H, Bignell GR, Cox C, et al. *Mutations of the BRAF gene in human cancer*. Nature. 2002 Jun 27;417(6892):949-54

Dazzi H, Hasleton PS, Thatcher N, et al (1990) *Malignant pleural mesothelioma and epidermal growth factor receptor (EGF-R). Relationship of EGF-R with histology and survival using fixed paraffin embedded tissue and the F4, monoclonal antibody*. Br J Cancer 61: 924–926.

De Luca A, Baldi A, Esposito V, et al., *The retinoblastoma gene family pRb/p105, p107, pRb2/p130 and simian virus-40 large T-antigen in human mesotheliomas.* Nat Med, 1997. 3(8): p. 913-6.

De Roock W, Claes B, Bernasconi, De Schutter J, et al. *Effects of KRAS, BRAF, NRAS, and PIK3CA mutations on the efficacy of cetuximab plus chemotherapy in chemo-refractory metastatic colorectal cancer: a retrospective Consortium analysis,* Lancet Oncol., 11 (8) (2010), pp. 753–762

Destro A, Ceresoli GL, Falleni M, et al. *EGFR overexpression in malignant pleural mesothelioma. An immunohistochemical and molecular study with clinico-pathological correlations.* Lung Cancer 2006;51:207–15.

Di Cristofano A, Pandolfi PP *The multiple roles of PTEN in tumor suppression*. Cell. 2000;100:387-90.

Di Nicolantonio, Arena S, Tabernero J et al. *Deregulation of the PI3K and KRAS signaling pathways in human cancer cells determines their response to everolimus*. Clin Invest. 2010;120:2858-66.

Dip R, Camenisch U, Naegeli H. *Mechanisms of DNA damage recognition and strand discrimination in human nucleotide excision repair*. DNA Repair 2004;3:1409–23.

Dote H, Tsukuda K, Toyooka S, et al, *Mutation analysis of the BRAF codon 599 in malignant pleural mesothelioma by enriched PCRRFLP*. Oncol Rep 2004;11:361–3.

Enomoto Y, Kasai T, Takeda M et al. *Epidermal growth factor receptor mutations in malignant pleural and peritoneal mesothelioma*. J Clin Pathol. 2012 Jun;65(6):522-7

Foddis R, De Rienzo A, Broccoli D, et al., *SV40 infection induces telomerase activity in human mesothelial cells.* Oncogene, 2002. 21(9): p. 1434-42.

Frattini M, Saletti P, Romagnani E, et al. *PTEN loss of expression predicts cetuximab efficacy in metastatic colorectal cancer patients*. Br J Cancer 2007;97:1139-45.

Garcia-Carbonero R, Paz-Ares L. *Systemic chemotherapy in the management of malignant peritoneal mesothelioma.* EJSO 2006;32:676-81.

Garland LL, Rankin C, Gandara DR, et al. *Phase II study of erlotinib in patients with malignant pleural mesothelioma: a Southwest Oncology Group Study*. J Clin Oncol 2007;25:2406–13.

Giovannetti E, Backus HH, Wouters D, et al, *Changes in the status of p53 affect drug sensitivity to thymidylate synthase (TS) inhibitors by altering TS levels*. Br J Cancer 2007 96:769-775.

Giovannetti E, Lemos C, Tekle C, Smid K, Nannizzi S, Rodriguez JA, et al. Molecular mechanisms underlying the synergistic interaction of erlotinib, an epidermal growth factor receptor tyrosine kinase inhibitor, with the multitargeted antifolate pemetrexed in non-small-cell lung cancer cells. Mol Pharmacol 2008;73:1290–1300.

Goey S, Eggermont A, Punt C, et al. *Intrapleural administration of interleukin 2 in pleural mesothelioma: a phase I-II study*. Br J Cancer 1995 72: 1283-1288.

Goldman ID, Zhao R: *Molecular, biochemical, and cellular pharmacology of pemetrexed.* Semin Oncol 2002;29:3-17.

Gomez HL, Santillana SL, Vallejos CS, et al: *A phase II trial of pemetrexed in advanced breast cancer: Clinical response and association with molecular target expression*. Clin Cancer Res 2006, 12:832-838.

Goodman JE, Nascarella MA, Valberg PA. *Ionizing radiation: a risk factor for mesothelioma*. Cancer Causes Control 2009, 20(8):1237-1254.

Gordon W Jr, Antman KH, Greenberger JS et al. *Radiation therapy in the management of patients with mesothelioma.* Int J Radiat Oncol Biol Phys. 1982;8:19-25.

Govindan R, Kratzke RA, Herndon 2nd JE, et al. Gefitinib in patients with malignant mesothelioma: a phase II study by the Cancer and Leukemia Group B. Clin Cancer Res 2005;11:2300–4.

Greaves, M. & Maley, C.C. *Clonal evolution in cancer*. Nature 481, 306-13 (2012).

Gridelli C, Bareschino MA, Schettino C, et al., Erlotinib in non-small cell lung cancer treatment: current status and future development, Oncologist, 12 2007, pp. 840–849.

Hanauske-Abel H, et al. In vitro chemosensitivity of freshly explanted tumor cells to pemetrexed is correlated with target gene expression. Invest New Drugs 2007;25:417–23
Hancock JF, *Ras proteins: different signals from different locations*. Nat Rev Mol Cell Biol. 2003 May;4(5):373-84. Review.

Harichand-Herdt S. and Ramalingam SS. *Targeted therapy for the treatment of Non-Small Cell Lung Cancer: focus on inhibition of Epidermal Growth Factor Receptor*. Semin Thorac Cardiovasc Surg 2008;20:217-23.

Hashimoto H, Ozeki Y, Sato M, Obara K, et al. *Significance of thymidylate synthase gene expression level in patients with adenocarcinoma of the lung*. Cancer 2006;106:1595–1601.

Heard E, *Recent advances in X-chromosome inactivation*. Curr Opin Cell Biol, 2004. 16(3): p. 247-55.

Hill RJ, Edwards RE, Carthew P, *Early changes in the pleural mesothelium following intrapleural inoculation of the mineral fibre erionite and the subsequent development of mesotheliomas.* J Exp Pathol Oxford 1990 71:105–118.

Hoeijmakers JH, *Genome maintenance mechanisms for preventing cancer* Nature, 411 (2001), pp. 366–374.

Holliday R Ageing: *X-chromosome reactivation*. Nature (Lond.) 1987 327:661-662.

Huynh KD, Lee JT, *Inheritance of a pre-inactivated paternal X chromosome in early mouse embryos*. Nature, 2003. 426(6968): p. 857-62.

Hynes NE, Lane HA. *ERBB receptors and cancer: the complexity of targeted inhibitors*. Nat Rev Cancer 2005;5:341–54.

J Clin Oncol. 2003;2:2629-30.

Janne PA, Taffaro ML, Salgia R, et al. *Inhibition of epidermal growth factor receptor signaling in malignant pleural mesothelioma.* Cancer Res 2002 62: 5242-5247.

Jonker DJ, O'Callaghan CJ, Karapetis CS, et al (2007) *Cetuximab for the treatment of colorectal cancer*. N Engl J Med 357: 2040–2048.

Kamp DW, Israbian VA, Preusen SE, et al. *Asbestos causes DNA strand breaks in cultured pulmonary epithelial cells: role of iron-catalyzed free radicals*. Am J Physiol. 1995;268:471-80.

Kitamura F, Araki S, Suzuki Y, et al, *Assessment of the mutations of p53 suppressor gene and Ha- and Ki-ras oncogenes in malignant mesothelioma in relation to asbestos exposure: a study of 12 American patients*. Ind Health 2002;40:175–81.

Kosaka T, et al. *Mutations of the epidermal growth factor receptor gene in lung cancer: biological and clinical implications*. Cancer Res 2004;64:8919–23.

Krause DS, Van Etten RA, *Tyrosine kinases as targets for cancer therapy*. N. Engl. J. Med. 2005;353:172–87.

Kurai J, Chikumi H, Hashimoto K, et al (2012) *Therapeutic antitumor efficacy of antiepidermal growth factor receptor antibody, cetuximab, against malignant pleural mesothelioma*. Int J Oncol 41: 1610–1618.

Lafuma J, Morim M, Poncy JL, et al, *Mesothelioma induced by intrapleural injection of different types of fibres in rats; synergistic effect of other carcinogens.* IARC Sci Publ, 1980(30): p. 311-20.

Lee C, Bayman N, Swindell R, et al. *Prophylactic radiotherapy to intervention sites in mesothelioma: a systematic review and survey of UK practice*. Lung Cancer Epub ahead of print, 2009.

Lee JT, Davidow LS, Warshawsky D, *Tsix, a gene antisense to Xist at the X-inactivation centre*. Nat Genet, 1999. 21(4): p. 400-4.

Lee JW, Soung YH, Kim SY, et al. *Somatic mutations of EGFR gene in squamous cell carcinoma of the head and neck*. Clin Cancer Res 2005;11:2879e82.

Lord R., Brabender J., Gandara D., et al. *Low ERCC1 expression correlates with prolonged survival after cisplatin plus gemcitabine chemotherapy in NSCLC*. 2002; 8:2286-91

Lord RVN, Brabender J, Gandara D, et al. *Low ERCC1 expression correlates with prolonged survival after cisplatin plus gemcitabine chemotherapy in non-small cell lung cancer*. Clin Cancer Res 2002;8:2286–2291.

Lynch TJ, Bell DW, Sordella R, et al. *Activating mutations in the epidermal growth factor receptor underlying responsiveness of non- small-cell lung cancer to gefitinib,* N Engl J Med 2004;350:2129e39.

Lyon MF, *Gene action in the X-chromosome of the mouse*, Nature (Lond.), 1961, 190: 372-373.

Lyon MF, *The William Allan Memorial Award address: X-chromosome inactivation and the location and expression of X-linked genes,* Am. J. Hum. Genet. 1988 42: 8-16.

Martin GR, Epstein CJ, Travis B , et al. *X-chromosome inactivation during differ entiation of female teratocarcinoma stem cells in vitro*. Nature (Lond.), 1978 271: 329-333.

Mendelsohn J, Baselga J, *Status of epidermal growth factor receptor antagonists in the biology and treatment of cancer*. J Clin Oncol 2003;21:2787—99.

Metcalf RA, Welsh JA, Bennett WP, et al. *P53 and Kirsten-ras mutations in human mesothelioma cell lines.* Cancer Res 1992;52:2610–5.

Metzger R, Leichman CG, Danenberg KD, et al. *ERCC1 mRNA levels complement thymidylate synthase mRNA levels in predicting response and survival for gastric cancer patients receiving combination cisplatin and fluorouracil chemotherapy*. J Clin Oncol 1998;16:309–316.

Mita MM, Mita A, Rowinsky EK. *The molecular target of rapamycin (mTOR) as a therapeutic target against cancer.* Cancer Biol Ther. 2003;2:S169-77.

Molinari F, Felicioni L, Buscarino M, et al (2011) Increased detection *sensitivity for KRAS mutations enhances the prediction of anti-EGFR monoclonal antibody resistance in metastatic colorectal cancer*. Clin Cancer Res 17: 4901–4914.

Montanaro F, Rosato R, Gangemi M, et al., *Survival of pleural malignant mesothelioma in Italy: a population-based study*. Int J Cancer. 2009 Jan 1;124(1):201-7. doi: 10.1002/ijc.23874.

Mossman BT, Bignon M, Corn M, et al, *Asbestos: Scientific developments and implication for public policy.* Science 1990, 247:294-301.

Murthy SS, et al. Expression of GPC3, an X-linked recessive overgrowth gene, is silenced in malignant mesothelioma. Oncogene 2000 19, 410-6.

Mukesh K. Nyati, Meredith A et al. *Integration of EGFR inhibitors with radiochemotherapy* Nature Reviews Cancer 6,876-88, 2006

Novelli M, Cossu A, Oukrif D, et al. *X-inactivation patch size in human female tissue confounds the assessment of tumor clonality*. Proc Natl Acad Sci U S A 2003, 100, 3311-4.

Nowak AK, Byrne MJ, Williamson R, et al. *A multicentre phase II study of cisplatin and gemcitabine for malignant mesothelioma.* Br J Cancer 2002, 87: 491-496.

Nyati MK, Morgan MA, Feng FY et al, Integration of EGFR inhibitors with radiochemotherapy, Nature Reviews Cancer, 2006 6, 876-88.

Ogawa Y, Lee JT, Xite, *X-inactivation intergenic transcription elements that regulate the probability of choice*. Mol Cell, 2003. 11(3): p. 731-43.

Okamoto I, et al., *Epigenetic dynamics of imprinted X inactivation during early mouse development*. Science, 2004. 303(5658): p. 644-9.

Okuda K, Sasaki H, Kawano O, et al. *Epidermal growth factor receptor gene mutation, amplification and protein expression in malignant pleural mesothelioma*. J Cancer Res Clin Oncol. 2008;134:1105-11.

Olaussen KA, Dunant A, Fouret P, et al. *DNA repair by ERCC1 in non-small-cell lung cancer and cisplatin-based adjuvant chemotherapy*. N Engl J Med 2006 355:983-991.

Paez J, *PI3K/PTEN/AKT pathway*, 2000.

Paez JG, Janne PA, Lee JC, et al. *EGFR mutations in lung cancer: correlation with clinical response to gefitinib therapy*. Science 2004;304:1497e500.

Parra HS, Tixi L, Latteri F, et al. *Combined regimen of cisplatin, doxorubicin, and alpha-2b interferon in the treatment of advanced malignant pleural mesothelioma: a Phase II multicenter trial of the Italian Group on Rare Tumors (GITR) and the Italian Lung Cancer Task Force (FONICAP)* Cancer 2001 92: 650-656.

Parsons BL, *Many different tumor types have polyclonal tumor origin: evidence and implications*. Mutant Res 659, 2008, 232-47.

Pass HI. *Malignant pleural mesothelioma: surgical roles and novel therapies*. Clin Lung Cancer. 2001;3:102-17.

Penny, G.D., et al., *Requirement for Xist in X chromosome inactivation*. Nature, 1996. 379(6561): p. 131-7.

Peto J, Decarli A, La Vecchia C, et al. *The European mesothelioma epidemic*. Br J Cancer. 1999;79:666-72.

Pollock PM, Harper UL, Hansen KS, et al. *High frequency of BRAF mutations in nevi*. Nat Genet. 2003;33:19–20

Prchal JT, Prachal JF, Belickova M, et al., *Clonal stability of blood cell lineages indicated by X-chromosomal transcriptional polymorphism*. J Exp Med, 1996. 183(2): p. 561-7.

Qi F, Okimoto G, Jube S, et al *Continuous exposure to chrysotile asbestos can cause transformation of human mesothelial cells via HMGB1 and TNF-α signaling.* Am J Pathol.2013 Nov;183(5):1654-66.

Rena O, Boldorini LR, Gaudino E, et al. *Epidermal growth factor receptor overexpression in malignant pleural mesothelioma: Prognostic correlations.* J Surg Oncol. 2011;104(6):701-5.

Rice D. *Surgical therapy of mesothelioma. Recent Results* Cancer Res. 2011;189:97-125.

Righi L, Papotti MG, Ceppi P, et al. *Thymidylate synthase but not excision repair cross-complementation group 1 tumor expression predicts outcome in patients with malignant pleural mesothelioma treated with pemetrexed-based chemotherapy*. J Clin Oncol. 2010;28:1534-9.

Robinson BW, Lake RA. *Advances in malignant mesothelioma*. N Engl J Med. 2005;353:1591-603

Robinson C, Callow M, Stevenson S, et al. *Serologic responses in patients with malignant mesothelioma: evidence for both public and private specificities*. Am J Respir Cell Mol Biol 2000, 22: 550-556.

Rose MG, Farrell MP, Schmitz JC: *Thymidylate synthase: A critical target for cancer chemotherapy*. Clin Colorectal Cancer 2002 1:220-229.

Rusch V, Saltz L, Venkatraman E, et al. *A phase II trial of pleurectomy/decortication followed by intrapleural and systemic chemotherapy for malignant pleural mesothelioma.* J Clin Oncol.1994;12:1156-63.

Rusch VW. *A proposed new international TNM staging system for malignant pleural mesothelioma: from the International Mesothelioma Interest Group*. Chest 1995;108:1122-28.

Rusch VW. *Pemetrexed and cisplatin for malignant pleural mesothelioma: a new standard of care?*

Sado T, et al., *Regulation of imprinted X-chromosome inactivation in mice by Tsix*. Development, 2001. 128(8): p. 1275-86.

Saltz LB, Meropol NJ, Loehrer PJ Sr, et al., *Phase II trial of cetuximab in patients with refractory colorectal cancer that expresses the epidermal growth factor receptor,* J. Clin. Oncol., 22 2004, pp. 1201–1208.

Samuels Y, Wang Z, Bardelli A, et al. *High frequency of mutations of the PIK3CA gene in human cancers.* Science. 2004;304:554.

Sancar A. *DNA repair in humans*. Annu Rev Genet 1995;29:69–105.

Santoro A, Cavina R, Latteri F, et al. *Activity of a specific inhibitor, gefitinib (IressaTM, ZD1839), of epidermal growth factor receptor in refractory non-small-cell lung cancer*. Ann Oncol 2004;15:33—7.

Schutte W, Blankenburg T, Lauerwald K, et al. *A multicenter phase II study of gemcitabine and oxaliplatin for malignant pleural mesothelioma.* Clin Lung Cancer 2003, 4: 294-297.

Seeker-Walker LM, *The meaning of a clone*. Cancer Genet. Cytogenet 1985 16: 87-88.

Senan S. *Indications and limitations of radiotherapy in malignant pleural mesothelioma.* Curr Opin Oncol 15: 144-147, 2003.

Sharma SV, Bell DW, Settleman J, Haber DA. *Epidermal growth factor receptor mutations in lung cancer. Nat Rev Cancer* 2007;7:169-81.

Shigematsu, H. et al. *Clinical and biological features associated with epidermal growth factor receptor gene mutations in lung cancers*. J. Natl Cancer Inst. 2005;97:339–46

Shih C, Chen VJ, Gossett LS, et al. *LY231514, a pyrrolo[2,3-d]pyrimidine-based antifolate that inhibits multiple folate-requiring enzymes*. Cancer Res. 1997;57:1116-23.

Shih C, Chen VJ, Gossett LS, et al: *LY231514, a pyrrolo[2,3-d]pyrimidine-based antifolate that inhibits multiple folate-requiring enzymes*. Cancer Res 1997, 57:1116-1123

Shintani Y, Ohta M, Hirabayashi H, et al., *New prognostic indicator for non-small-cell lung cancer, quantitation of thymidylate synthase by real-time reverse transcription polymerase chain reaction*. Int J Cancer 2003;104:790–95.

Sigmond J, Backus HH, Wouters D, Temmink OH, et al. *Induction of resistance to the multitargeted antifolate Pemetrexed (ALIMTA) in WiDr human colon cancer cells is associated with thymidylate synthase overexpression*. Biochem Pharmacol 2003;66:431–8.

Sridhar SS, Seymour L, Shepherd FA, et al, *Inhibitors of epidermal-growth-factor receptors: a review of clinical research with a focus on non-small-cell lung cancer,* Lancet Oncol., 4 2003, pp. 397–406.

Strickler HD, Goedert JJ, Fleming M, et al. *Simian virus 40 and pleural mesothelioma in humans*. Cancer Epidemiol Biomarkers Prev. 1996;5:473-5.

Sugarbaker DJ, Flores RM, Jaklitsch MT, et al. *Resection margins, extrapleural nodal status, and cell type determine postoperative long-term survival in trimodality therapy of malignant pleural mesothelioma: results in 183 patients.* J Thorac Cardiovasc Surg 1999 117: 54-63.

Tan YH, Liu Y, Eu KW, et al. *Detection of BRAF V600E mutation by pyrosequencing. Pathology* 2008; 40 (3): 295–8.

Testa JR, Cheung M, Pei J, et al., *Germline BAP1 mutations predispose to malignant mesothelioma.* Nat Genet, 2011. 43(10): p. 1022-5.

Tilleman TR, Richards WG, Zellos L, et al. *Extrapleural pneumonectomy followed by intracavitary intraoperative hyperthermic cisplatin with pharmacologic cytoprotection for treatment of malignant pleural mesothelioma: a phase II prospective study*. J Thorac Cardiovasc Surg. 2009;138:405–11.

Velcheti V, Kasai Y, Viswanathan AK, et al (2009) *Absence of mutations in the epidermal growth factor receptor (EGFR) kinase domain in patients with mesothelioma*. J Thorac Oncol 4: 559.

U. Vogel, M. Dybdahl, G. Frentz et al, DNA repair capacity: inconsistency between effect of over-expression of five NER genes and the correlation to mRNA levels in primary lymphocytes, Mutation Research/DNA Repair Volume 461, Issue 3, 9 November 2000, 197–210.

Vecchione L, Jacobs B, Normanno N, Ciardiello F, Tejpar S. EGFR-targeted therapy. Exp Cell Res. 2011Nov 15;317(19):2765-71

Vickers MA, McLeod E, Spector TD et al (2001) Assessment of mechanism of acquired skewed X inactivation by analysis of twins. Blood 97: 1274–1281

Vogelzang NJ, Rusthoven JJ, Symanowski J, et al. *Phase III study of pemetrexed in combination with cisplatin versus cisplatin alone in patients with malignant pleural mesothelioma.* J Clin Oncol 2003, 21: 2636-2644.

Wagner JC, Skidmore JW, Hill RJ, et al., *Erionite exposure and mesotheliomas in rats.* Br J Cancer 1985 51:727–730.

Wan PT, Garnett MJ, Roe SM, *Mechanism of activation of the RAF-ERK signaling pathway by oncogenic mutations of B-RAF"*. Cancer Genome Project (March 2004). Cell 116 (6): 855–67.

Wang ZJ, Reddy GP, Gotway MB, et al. *Malignant pleural mesothelioma: evaluation with CT, MR imaging, and PET.* Radiographics 2004, 24: 105-119.

Wang, L. et al. *Somatic single hits inactivate the X-linked tumor suppressor FOXP3 in the prostate*. Cancer Cell 2009 16, 336-46.

Xin L, *Cells of origin for cancer: an updated view from prostate cancer*. Oncogene 32, 3655-63, 2013.

Yang H, Rivera Z, Jube S, et al., *Programmed necrosis induced by asbestos in human mesothelial cells causes high-mobility group box 1 protein release and resultant inflammation.* Proc Natl Acad Sci U S A, 2010. 107(28): p. 12611-6.

Yang H, Testa JR, Carbone M. *Mesothelioma epidemiology, carcinogenesis, and pathogenesis*. Curr Treat Options Oncol. 2008;9:147–57.

Yutaro Suzuki, Hideki Murakami, Koji Kawaguchi, et al. *Activation of the PI3KAKT pathway in human malignant mesothelioma cells*. Mol Med Rep 2009;2:181–8.

Zheng Z, Chen T, Li X, Haura E, Sharma A, Bepler G. *DNA synthesis and repair genes RRM1 and ERCC1 in lung cancer*. N Engl J Med. 2007;356:800-8.

Zucali PA, Giovannetti E, Destro A, et al. *Thymidylate synthase and excision repair cross-complementing group-1 as predictors of responsiveness in mesothelioma patients treated with pemetrexed/carboplatin*. Clin Cancer Res. 2011;17:2581-90.

Zuo T et al. *FOXP3 is an X-linked breast cancer suppressor gene and an important repressor of the HER-2/ErbB2 oncogene*. Cell 2007 129, 1275-86.